Ph.D. THESIS

Collapse Strength Prediction of ERW Pipes Subjected to External Pressure by Simulation Analysis of Manufacturing Process

외압을 받는 ERW 강관의 조관공정 모사해석을 통한 파괴 강도 평가

2020 년 2 월

서울대학교 대학원

건설환경공학부

한 성 욱

ABSTRACT

Collapse Strength Prediction of ERW Pipes Subjected to External Pressure by Simulation Analysis of Manufacturing Process

Seong-Wook Han
Department of Civil and Environmental Engineering
Seoul National University

Offshore pipeline is a major method of oil and gas transportation owing to its reliable strength against harsh environments including external pressure. As production of oil and gas in deep-water is increasing with the ongoing growth of the energy industry, demand for high structural performance pipes has become larger than ever and brought the attention on thicker pipes.

Among the various kinds of steel pipes, the electric resistance welded (ERW) pipes have traditionally been used for land pipelines, tubing and casing rather than for offshore pipelines due to the potential weakness of welded seams. As the welding technology has improved, however, recent studies have shown that the ERW pipe is also applicable to deep-water pipelines.

Compared with other types of steel pipes, the merits of the ERW pipe come from the manufacturing process. ERW pipes are fabricated along one linear continuous process from the plate to when the pipe is cut into desired lengths. This continuous manufacturing process of ERW pipes has the advantage of

increasing the productivity, but makes it difficult to track plastic deformation correctly during the manufacturing process. And then, the complicate histories of the plastic deformation generate the following problems.

First, the ERW pipe manufacturing process make material properties of the raw plate changed significantly. The repeated loading and unloading cycles conducted throughout the manufacturing process change the yield strength due to the modified stress-strain relationship by the Bauschinger effect and the strain hardening. The changed yield strength not only has a significant effect on the structural performance of the ERW pipe, but also is used a representative indicator for quality evaluation of the ERW pipe. Therefore, the accurate prediction of the material properties will result in benefits in terms of the cost and time spent for the repeated inspection, design and production to secure the enough structural performance of the pipe.

The second problem relates to the geometric imperfection and residual stress inherent to the repetitive plastic deformation and elastic spring back during the manufacturing process. Like the material properties, the out-of-roundness and residual stress of the pipe are dominant parameters determining its collapse pressure but generated in such an unpredictable manner that increase the design uncertainty. Loss of accuracy in the ERW pipe leads to excessively conservative design that does not guarantee the pipe to provide consistent quality and satisfactory structural performance.

This thesis evaluates the collapse performance of ERW pipes as following procedures. The procedure involves (1) the computational simulation of ERW

pipe manufacturing processes by three-dimensional finite element analysis to evaluate effects of the plastic deformation for prediction of yield strength, out-of-roundness and residual stress; (2) the collapse analysis of ERW pipes using the results of the manufacturing simulation; and, (3) parametric study to examine the effect of design variables such as diameter, thickness and sizing process on enhancement of collapse performance.

To improve the accuracy of the simulation of the ERW pipe manufacturing process, the combined nonlinear hardening model is incorporated to describe the plastic characteristics including yield plateau and evolution of Young's modulus as well as strain hardening and Bauschinger effect.

In the ERW pipe manufacturing process, finpass and sizing processes which make large deformation in the circumferential direction of the pipe are controlled as manufacturing variables. These manufacturing variables are defined as roll-forming and sizing ratios based on the girth history during the manufacturing, and variations of yield strength, out-of-roundness, and residual stresses are evaluated according to the manufacturing variables.

Collapse analysis is then performed using the pipe model after the ERW pipe manufacturing analysis, so that the result of the manufacturing process can be considered in collapse analysis. Parametric analysis is performed to investigate the effect of the sizing process on its yield strength, out-of-roundness and collapse performance.

It is found that larger sizing ratio has effect on improving the out-of-roundness and increasing the compressive yield strength but decreasing the

tensile yield strength. These effects lead to enhancement of the collapse performance, and the effect of the sizing ratio on enhancement of collapse performance increases for the smaller D/t.

The current design criteria do not consider the advantages of the sizing process on the collapse pressure. This lead that the difference between the analysis result and design criteria increases for a thicker pipe which is significantly influenced by the sizing process.

The developed analytical approach is expected to provide useful data for the manufacturing process enhancing the collapse performance and improving the quality of the ERW pipe.

Keywords: ERW pipe; Roll-forming; Sizing; Finite element analysis; Ovality; Yield strength; External pressure, Collapse pressure

Student Number: 2015-30287

TABLE OF CONTENTS

LIST OF FIGURES

LIST OF TABLES

CHAPTER 1

INTRODUCTION

1.1 Research background

Offshore pipeline is a major mean of oil and gas transportation owing to its reliable strength against harsh environments such as external pressure. As production of oil and gas in deep-water is increasing with the ongoing growth of the energy industry, demand for high structural performance pipes has become larger than ever and brought the attention on thicker pipes.

Among the various kinds of steel pipes, the electric resistance welded (ERW) pipes has traditionally been used for land pipelines rather than for offshore pipelines due to the potential weakness of welded seams. As the welding technology has improved, however, recent studies have shown that ERW pipe is also applicable to deep-water pipelines (Nagata et al., 2016; Tsuru et al., 2015).

Compared with other types of steel pipes, the merits of ERW pipe come from the manufacturing process. The manufacturing process of ERW pipe can be divided into five steps, each with the potential to cause plastic deformations: Uncoiling, leveling, roll-forming, welding, and sizing processes (Nishimura et al., 1997). Uncoiling and leveling are the processes that are used to unfold and flatten rolled steel sheets from steel mills. Roll-forming is a process whereby a steel plate is rolled into a circular pipe shape,

welding joins the two opposing edges to form a pipe, and sizing is the process of applying compression to the pipe following the welding to optimize the circular shape. These five steps are performed along one linear continuous process from the plate to when the pipe is cut into desired lengths, and these steps lead to ERW pipe with smaller deviations in diameter and thickness in the circumferential direction compared with other types of pipe such as UOE and spiral pipes. These manufacturing steps make ERW pipe more cost-effective because uniform thickness reduces the net weight, and relatively smaller deviations in diameter and uniform thickness increase the girth welding speed that is required either in the field or on a lay-barge (Kyriakides and Corona, 1991).

In spite of their merits, ERW pipes present still concerns regarding their structural performance (Kyriakides et al., 1991; Herynk et al., 2007). The continuous manufacturing process of ERW pipes has the advantage of increasing the productivity, but makes it difficult to track changes in geometric information or yield strength during the manufacturing. These changes have also significant effects on the structural performance of the pipe, and still make ERW pipe research challenging.

The influence factors on the collapse pressure of steel pipes have been examined in numerous previous studies (Yeh and Kyriakides, 1986; Murphey and Langner, 1985). In the case of thick pipes experiencing buckling in the plastic range, the material properties, diameter-to-thickness ratio (D/t), geometric imperfections, and residual stress were found to be the most

important parameters influencing the structural performance. Except for the D/t, those factors are essentially affected by the plastic deformations performed in the pipe forming process (Qiang et al, 2015; Tianxia et al, 2016).

The stress-strain relationship of the ERW pipes is significantly changed from that of the raw plate because of the strain hardening and Bauschinger effect related to the complicated plastic strain hysteresis (Lee et al., 2017). The material properties of steel pipes are not only variables that have a sensitive effect on the structural performance of steel pipes, but also are representative indices of a quality evaluation for steel pipes (API, 2012). Therefore, inaccurate prediction of the material properties will result in lower strength and structural performance of the pipe and will lead to tremendous cost and time spent for the repeated inspection, design, and manufacturing tasks. Furthermore, the plastic deformation at each manufacturing step exerts direct effects on the subsequent manufacturing step. However, the geometric imperfections and residual stress occur with high degree of uncertainty that their assessment at the design stage has become a challenging task due to their critical effect on the structural performance of the pipe like the collapse pressure (Aiman et al., 2008; Moen et al., 2008). The excessively conservative material properties and cross-sectional design due to these uncertain factors not only lead to increasing cost and time consumption, but also mean that the steel pipe design cannot guarantee consistent and satisfactory quality.

In absence of straightforward ways to derive these key design parameters analytically, conventional pipe design had to rely on their own know-how obtained by trial-and-error experience. Such approach, however, is far from being consistent in securing the desired yield strength, structural performance and productivity of the pipe despite the same steel pipe. There is thus a pressing need for a standard design method based on the accurate prediction of the yield strength and structural performance of the formed steel pipes.

1.2 Literature review

As the demand for ERW pipe increases, higher accuracy in evaluating strength is now required to satisfy the design limit state, and one of the main considerations for the design of deep-water pipelines is to ensure resistance to external pressure. The collapse performance of a pipe against external pressure could be affected by factors that include material and geometric properties, as well as residual stress (Bastola et al., 2015; Fraldi and Guarracino, 2013).

During the manufacturing of ERW pipes, significant deformation could be caused by repetitive loading and unloading. Kyriakides and Corona (2007) conducted finite element analysis and confirmed that the Bauschinger effect should be considered the elastic-perfectly plastic stress–strain relationship or else the collapse performance can be overestimated. They also confirmed that the collapse performance could be enhanced by improving the out-of-

roundness of the cross-section. Bastola et al. (2014) conducted finite element analysis and confirmed that residual stress could reduce the collapse pressure by as much as 20%, and that the residual stress along the circumferential direction of the pipe were more significant on collapse performance than those along the longitudinal direction.

Factors such as out-of-roundness and residual stress could be determined during the manufacturing, particularly during the roll-forming and sizing processes. Since modification to the configurations and arrangements of the rolls is difficult to investigate, it is difficult to experimentally verify the influence of the manufacturing process on these factors. Thus, finite element analysis that can accurately simulate the manufacturing process is necessary. The aforementioned studies (Bastola et al., 2015; Fraldi and Guarracino, 2013; Kyriakides and Corona, 2007), however, forcibly imposed such factors to their finite element model without simulating the manufacturing process, so that it is questionable whether the results can be considered realistically. Several studies (Lee et al., 2017; Nishimura et al., 1997; Yi 2017) have investigated the effect of the manufacturing process on out-of-roundness or residual stress, but these studies did not simulate all steps in the manufacturing processes or had limitations in the adopted material model. These over-simplified approaches are understandable because numerically simulating the manufacturing process demands complex analysis following excessive computational effort.

1.3 Research objective and scope

This thesis intends to evaluate the collapse performance of ERW pipes considering the ERW pipe manufacturing process. The proposed procedure involves the computational simulation of the ERW pipe manufacturing process and the structural performance analysis reflecting the results from simulation to predict the collapse pressure of the pipes.

As a first step, ERW pipe manufacturing processes are simulated using three-dimensional finite element method to track the development of the yield strength of the pipes throughout the multi-stage pipe forming process. For the simulation, the combined nonlinear hardening model considering the strain hardening, the Bauschinger effect, the yield plateau and the evolution of Young's modulus is adopted to describe the complicated plastic behaviors of steel due to repeated loading and unloading during the manufacturing process.

The simulation can track the stress and strain histories during whole manufacturing process and investigate the yield strength, geometric imperfections and residual stress of the pipe after the manufacturing. In the following step, the collapse pressure known to be the principal structural performance indicators for offshore pipes are evaluated using the FEA model after the manufacturing process analysis.

This study conducts extensive parametric analysis to examine the effect of two major design variables that are 1) diameter to thickness ratio, 2) sizing

ratio on the yield strength, the out-of-roundness, residual stress and collapse performance of the pipe.

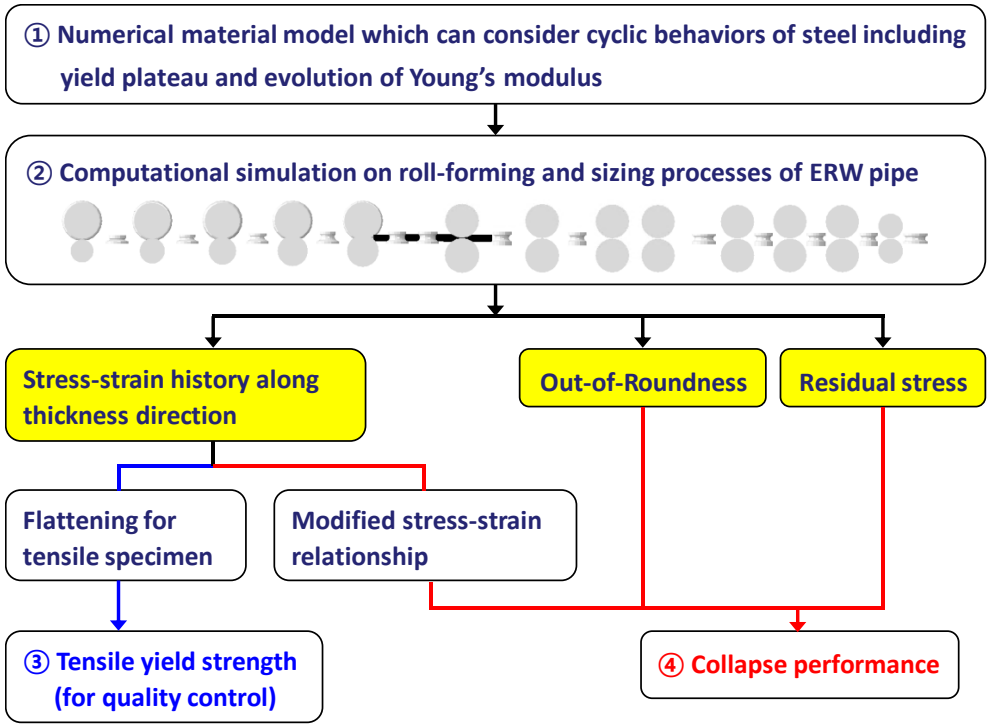

Fig. 1.1. Flow chart for prediction of yield strength and collapse performance of the pipe

1.4 Outline of the thesis

This thesis is organized into six chapters and structured in order to introduce each parts of the proposed framework.

In this chapter, the background of this work and the brief introduction of the proposed framework are described. Several related previous studies are also reviewed.

Next, in Chapter 2, the simulation of the ERW pipe manufacturing process using three-dimensional finite element analysis is introduced. The establishment and specifications of the numerical material model based on combined hardening model for the computational simulation of the ERW pipe manufacturing process are described. The features and roles of the simulated processes are introduced, and the contact and boundary conditions between rollers and plate are carefully considered. Finally, for the reliability of the analytical model, convergence checks on time increment and mesh size are performed.

Chapter 3 introduces quality evaluation of the ERW pipe. The adjustable manufacturing conditions, which are the roll-forming and sizing ratios, are defined based on the geometric deformation history. By controlling these two manufacturing conditions, the variations of out-of-roundness and residual stress after the manufacturing are evaluated. Also, the changes in the tensile and compressive yield strength after the manufacturing due to repetitive

loading and unloading are evaluated. In particular, the simulation of the flattening process is considered for tensile tests.

Chapter 4 introduces the prediction of the collapse performance to reflect the manufacturing process of ERW pipe. The effects of influence factors such as out-of-roundness, residual stress and compressive yield strength on collapse performance are evaluated separately. Variations of the influence factors by the sizing process lead to change in the collapse performance. It is revealed that the collapse performance can be enhanced by adjusting the sizing process.

Chapter 5 investigates the influence of key design variables on the collapse performance through parametric study with practical and feasible values and ranges of the parameters. The key variables on collapse performance are identified and their influence on the collapse pressure is discussed. And the analysis results are compared with the design criteria to investigate the advantage of the ERW pipe manufacturing process.

Finally, in Chapter 6 presents a summary of the major findings of this study and describes areas where further study is needed.

CHAPTER 2

SIMULATION OF ERW PIPE MANUFACTURING PROCESS USING THREE-DIMENSIONAL FINITE ELEMENT ANALYSIS

Unlike the small deformation problem, for the large deformation problem such as manufacturing process of pipes, there is no specific stress at a specific strain due to path dependency. In other words, the large deformation problem is an ill-posed problem with geometric nonlinearity, material nonlinearity and boundary nonlinearity, and requires careful consideration of the analysis results. In order to verify the results of large deformation analysis, it is best to compare the analysis results with the experimental results. However, due to the characteristics of the ERW steel pipe manufacturing process in Korea, there is a limit to the verification using the experimental results.

In this chapter, it was attempted to simulate the manufacturing process of the ERW pipe to reflect the actual behavior as much as possible.

2.1 Numerical material model in simulation

During the whole pipe manufacturing process, the material undergoes elastic-plastic deformations including repeated load reversals. As shown in Fig. 2.1,

Therefore, the accurate material modeling is of major importance for the reliable prediction of yield strength of the pipe. For that, refined numerical material model which describes the elastic-plastic behaviors including work hardening and Bauschinger effect is required. In this thesis, the modified Chaboche model (Zou et al, 2016) is adopted as a constitutive model. It modified original Chaboche model to have flexibility for wide range of material characteristics. Apart from work hardening and Bauschinger effect, it is capable of representing clear yield plateau and evolution of Young's modulus. On the other hand, uniaxial tension test was performed to calibrate material parameters of the model.

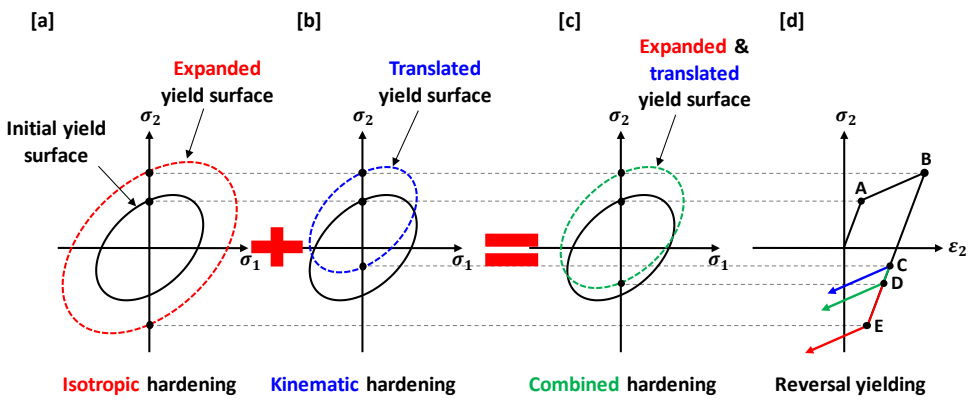

Fig. 2.1. Change in yield strength by isotropic and kinematic hardenings

2.1.1 Constitutive model

The Von mises yield function with kinematic and isotropic hardening is defined by Equation (2.1).

$$f = \|\sigma - \chi\| - \eta = 0 \tag{2.1}$$

In Equation 2.1, σ is the stress and χ and η are the terms related to kinematic and isotropic hardening, respectively, indicating the translation and expansion of the yield surface. The stress, σ, is defined by Equation (2.2).

In Equation (2.2), χ_k, is composed of three stress components. Equation (2.3) defines the backstress.

$$\sigma = \sum_{k=1}^{3} \chi_k \pm \eta \tag{2.2}$$

$$\chi_k = \pm\frac{C_k}{\gamma_k} + \left(\chi_{k0} \mp \frac{C_k}{\gamma_k}\right) exp\left(-\gamma_k\left|\varepsilon_p - \varepsilon_{p0}\right|\right) \tag{2.3}$$

In Equation (2.3), C_k and γ_k are the material hardening terms, ε_p is the plastic strain, χ_{k0} and ε_{p0} refer to χ_k and ε_p at the beginning of the roll-forming and sizing processes, respectively. The steel that underwent plastic deformation has no yield plateau according to the Bauschinger effect. Equation (2.4) shows that yield plateau is expressed by dividing the plastic section of the isotropic hardening term by the accumulative plastic strain.

$$\eta = \begin{cases} \sigma_0 + (\sigma_a - \sigma_0) \cdot \left(1 - exp(-b_a p)\right), p \leq \Delta\varepsilon_{pla} \\ \psi + Q \cdot \left(1 - exp(-bp)\right), p \geq \Delta\varepsilon_{pla} \end{cases} \tag{2.1}$$

In Equation (2.4), Q, σ_0, and $\Delta\varepsilon_{pla}$ represent the saturated isotropic hardening stress, the initial yield strength, and the length of the yield plateau, respectively. σ_a, b_a, and ψ are the material parameters for simulating the yield plateau and p is the accumulative plastic strain.

Consideration of springback is essential when large deformation occurs, and the springback is affected not only by the Bauschinger effect but also by Young's modulus (Yoshida, 2002). Equation (2.5) shows the decrease in Young's modulus according to accumulative plastic strain.

$$E(p) = E_0 - (E_0 - E_a)[1 - exp(-\xi p)] \tag{2.2}$$

In Equation (2.5), E_0 and E_a are the Young's modulus of the plate and the reduced Young's modulus at the infinitely large accumulated plastic strain, respectively. ξ is the material coefficient, and the Young's modulus reduces E_a from the initial E_0 according to the accumulative plastic strain during the roll-forming process.

2.1.2 Validation of material model

The investigated pipe was constructed of API 5L X70 steel. A dog bone specimen was taken from the actual steel sheet. A 2% tension-compression-tension cyclic loading test was carried out as shown in Fig. 2.2. The material coefficients of the Modified Chaboche model were calibrated to the test results using the least-square method combined with a genetic algorithm, as follows: $E_0 = 216277.2$ MPa , $\sigma_0 = 539.6$ MPa , $\Delta\varepsilon_{pla} = 0.00957$, $E_a = 200000$ MPa , $\xi = 186.5$, $Q = 184.5$ MPa , $\sigma_a = 379.2$ MPa , $C_1 = 20535.2$, $C_2 = 33855.9$, $C_3 = 999.6$, $\gamma_1 = 420.8$, $\gamma_2 = 255.6$, $\gamma_3 = 3.7$, $b = 52.7$, and $b_a = 225.5$.

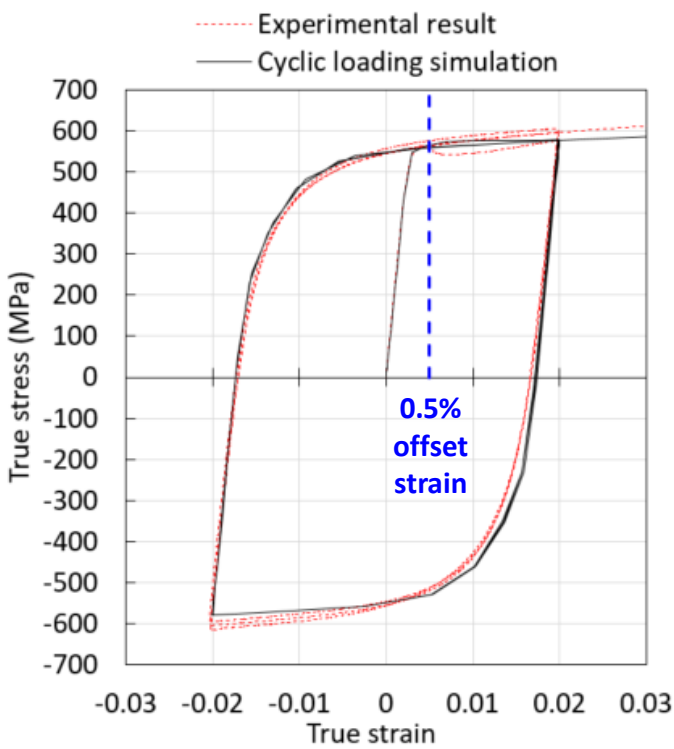

Fig. 2.2. Validation of the adopted material model for API 5L X70 steel

2.2 Description of the ERW pipe manufacturing process

The ERW pipe manufacturing process in this study can be divided into two parts. In the first part, the plate is formed in a circular shape before welding process. The second part is compressing the pipe after welding. It is necessary to investigate the role of each part.

2.2.1 Roll-forming and sizing processes

The roll-forming process is a shape in which the plate is rolled into a circular shape just before welding. The roll-forming process can be classified into two types. The first is breakdown, forming both edges of the plate. Breakdown roller is composed of up and down roller as shown in Fig. 2.3a. The breakdown consists of a set of five upper and lower rollers, and the width in the upper rollers are gradually reduced to form the edge of the plate. Since the welding surfaces of both ends are not constrained during the breakdown process, it is formed in the free bending state. Therefore, the length of the neutral layer is formed while maintaining the same length as the plate width before the breakdown process. The role of the left and right rollers disposed between the upper and lower rollers prevents the formed edges from excessively opening due to the springback after the rollers pass through the rollers.

The edge-formed plate through breakdown enters the finpass process. As shown in Fig. 2.3b, the finpass rollers increase the thickness of the weld surface by contact the weld surface with the fins at the upper of the roller. In addition, it obtains the cleanliness of the welding surface by contacting with fin in order to improve the quality of the welding. The finpass is composed of three upper and lower rollers, and the fin width of the upper roller decreases gradually as shown in Fig 2.3b. In other words, the fin angle is gradually decreased to make the plate close to the circle after breakdown until just before welding.

2.2.2 Sizing process

The sizing process is to improve the out-of-roundess and straightness of the steel pipe after welding. It also serves to match the diameter of the target steel pipe. As shown in Fig. 2.3d, one set of sizing rollers consists of upper and lower rollers, like the breakdown and the finpass roller. The sizing process consists of a total of four roller sets. The sizing rollers reduce the size of the steel pipe by gradually decreasing the size of the rollers at a constant rate. In addition, the left and right roller sets placed between the four upper and lower roller sets alleviate the springback effect, and serve as a guide for the plate to pass through correctly.

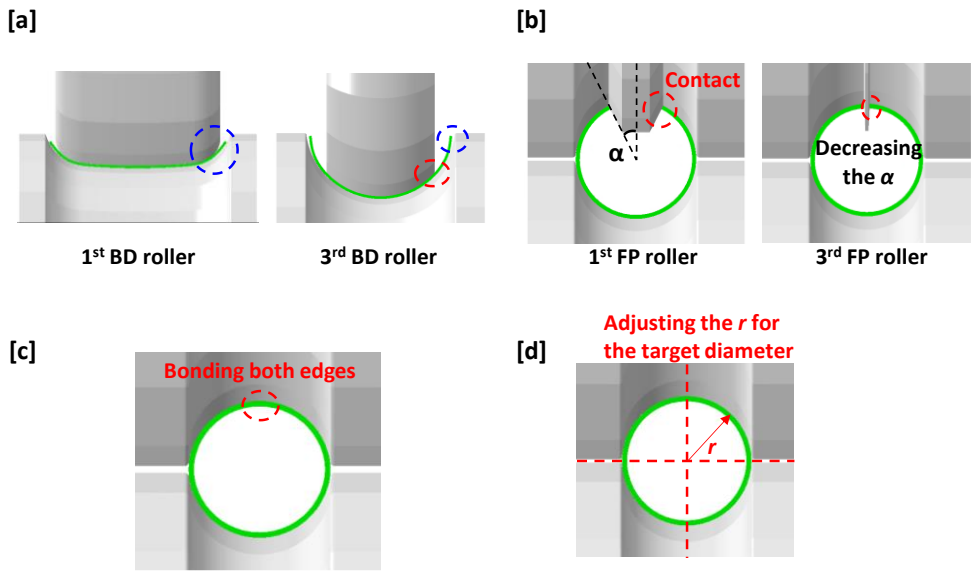

Fig. 2.3. Shape of the rollers composing the ERW pipe manufacturing process: (a) breakdown, (b) finpass, (c) squeezing, and (d) sizing

2.3 Details of finite element analysis simulation

The three-dimensional finite element analysis in this study was performed using ABAQUS 2018, a commercial program. The pipe manufacturing process simulated by moving the roller while fixing the plate as opposed to the actual pipe manufacturing process where the roller is fixed and the plate moves. Rollers and plates were simulated as rigid bodies and solid elements, respectively, and solid element modeling the pipe incorporates eight nodes with linear and reduced integration with an isoparametric formulation, which is referred to as C3D8R in ABAQUS.

In addition, the contact condition between the plate and the roller is one of the most important factors in the ERW pipe manufacturing process simulation because the plate is formed depending on the shape of the rollers. In other words, the difference in the deformation history during the manufacturing can be generated according to the contact conditions, not only the quality of the pipe after the tube can be properly secured, but also can not accurately simulate the actual pipe manufacturing condition. The contact conditions considered in the simulation are divided into two types. The one is the contact between the roller and the plate to be considered throughout the whole pipe manufacturing process. The other is between the welding surfaces of the plate. The simulation of ERW pipe manufacturing process is shown in Fig. 2.4.

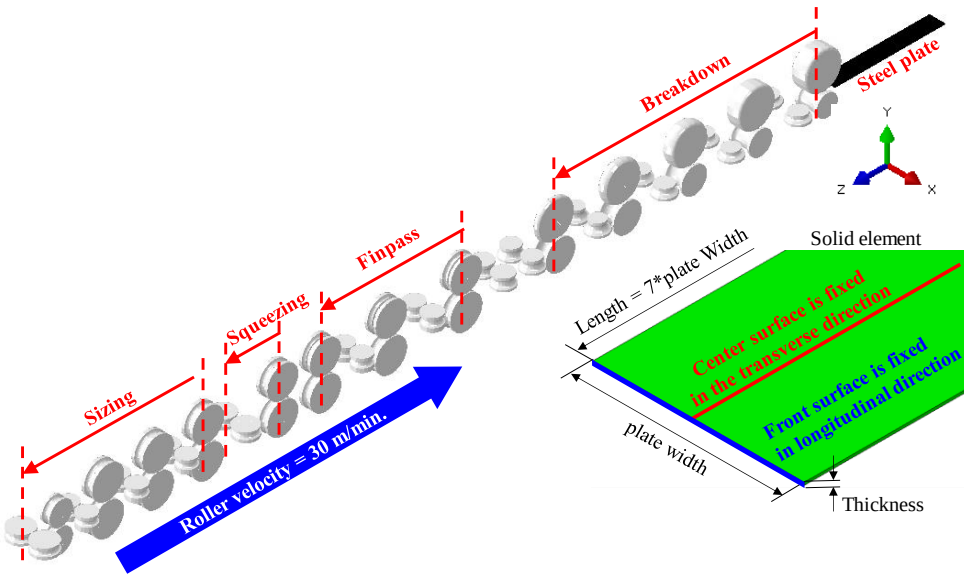

Fig. 2.4. Simulation of ERW pipe manufacturing process

2.3.1 Boundary conditions

In contrast to the actual pipe manufacturing process conditions, in this simulation, the plate was fixed and the roller was moved. As shown in Fig. 2.4, the roller was moved in the z-direction, which along the longitudinal direction of the plate, and the moving speed of the roller was 30 m/minute, which corresponds to the pipe production speed in the manufacturing company.

In order to fix the plate in the direction of roller movement, the front surface of the plate was fixed in the z-direction. In addition, the surface of mid-section in the transverse direction of the plate was fixed in the x-direction so that the symmetrical simulation was performed.

2.3.2 Contact conditions between rollers and steel plate

The roller and plate are set to prevent penetration each other. Also, the friction coefficient between the plates and the rollers was assumed as 0.15. Since the coefficient of friction is complexly determined by the roller moving speed, the surface roughness of the rollers, and the lubricant, it is different for each pipe manufacturing company. In this study, friction coefficient 0.15 was determined as shown in Fig. 2.5a.

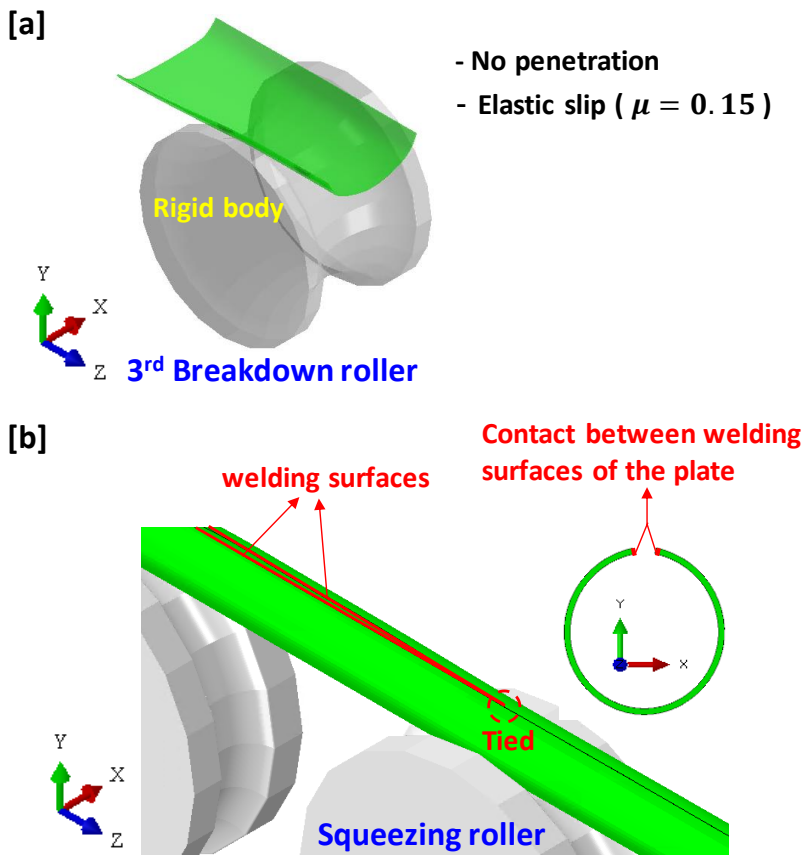

Fig. 2.5. Contact conditions in simulation: (a) between rollers and plate, and (b) between welding surfaces

2.3.3 Contact conditions between welding surfaces of steel plate

Welding simulation is required between the roll-forming and the sizing processes because it is done in one step until the manufacturing process is completed. In this study, however, the welding process is considered only to attach the welding surfaces between the last finpass and the first sizing rollers as shown in Fig. 2.5b. Once the two welding surfaces are in contact with each other, the tie condition is set to tie. In addition, once contact was made, separation and slip is not allowed.

2.4 Convergence of three-dimensional finite element analysis

This three-dimensional finite element analysis was carried out by explicit method. In order to ensure the reliability of the analysis results, it is better to simulate the actual behavior as closely as possible by decreasing the time increment and the size of the mesh. However, as the time increment and mesh size get smaller, the analysis time increases, so the appropriate time increment and mesh size should be determined. In other words, it is necessary to stabilize the analysis model to examine the time increment and mesh size that converge the analysis results.

2.4.1 Time increment for dynamic explicit analysis

It is necessary to examine whether the convergence of analysis results is secured according to the time increment of explicit analysis. In an explicit analysis, the stable time increment is determined by the size of the element and the type of material. That is, the smaller the mesh size, the lower the rigidity of the material or the higher the density, the larger the stable time increment.

As shown in Fig. 2.6, the stress histories during the manufacturing process are examined for two different time increments. The stress history was evaluated at the innermost and outermost layers at the opposite line of the seam weld, and the evaluation was carried out at the mid-section of the plate. First, stress history was evaluated for two Δt which are 4.0×10^{-6} and 2.0×10^{-6}. The difference between the two stress histories is minor until the breakdown, but The difference in stress history started from the finpass process. After sizing, the residual stresses have about twice the difference. This is because the convergence cannot be secured for the compression in the circumferential direction of the pipe after the finpass, and errors have accumulated continuously.

Fig. 2.7, the time increment was reduced from 4.0×10^{-6} to 2.2×10^{-6} and compared with the stress history of 2.0×10^{-6}. Unlike the results in Fig. 2.6, the difference in stress history is reduced. However, the difference in stress history after the finpass still occurred.

Fig. 2.8, the time increment was reduced from 2.0×10^{-6} to 1.8×10^{-6} and compared with the stress history of 2.0×10^{-6}. Unlike the results in Figs. 2.6 and 2.7, the difference in stress history was insignificant, and the residual stress after piping was almost the same. The results in this study are analyzed assuming a time increment of 2.0×10^{-6}.

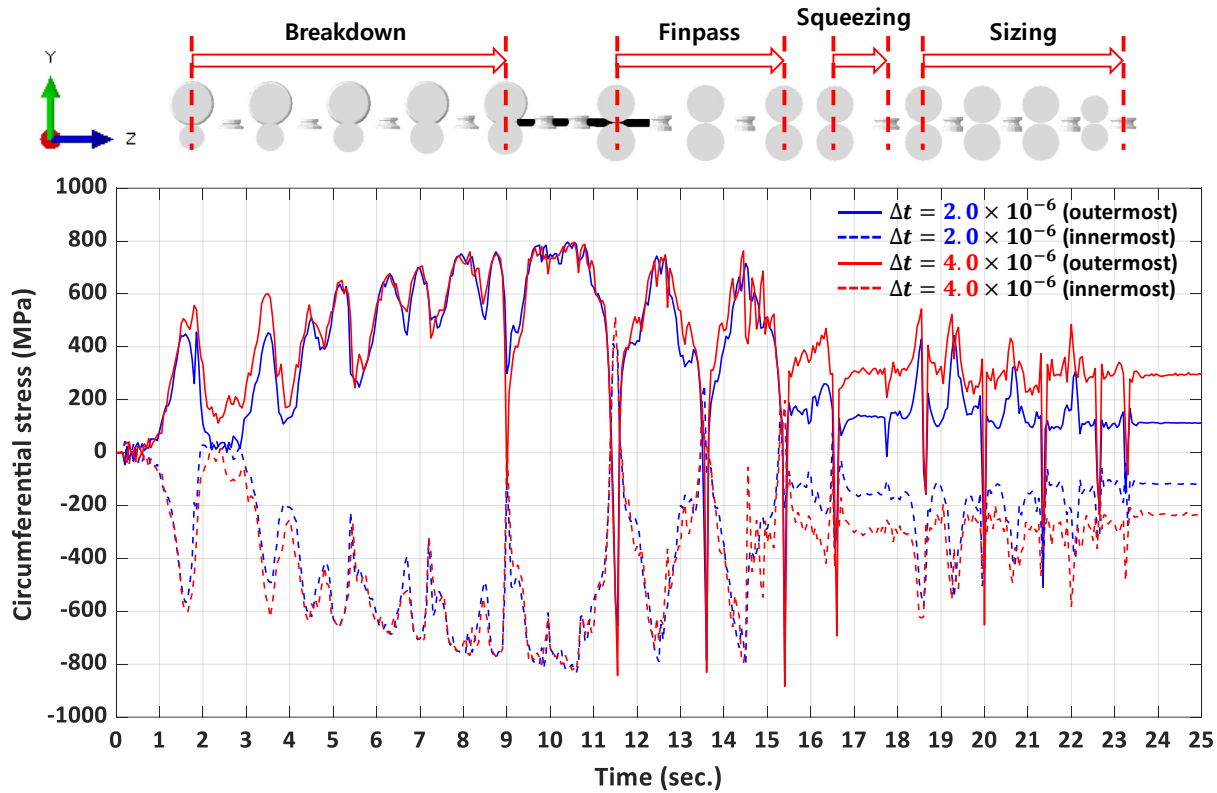

Fig. 2.6. Stress history during the manufacturing process at the opposite line of the seam weld:

$$\Delta t = 2.0 \times 10^{-6} \text{ vs } \Delta t = 4.0 \times 10^{-6}$$

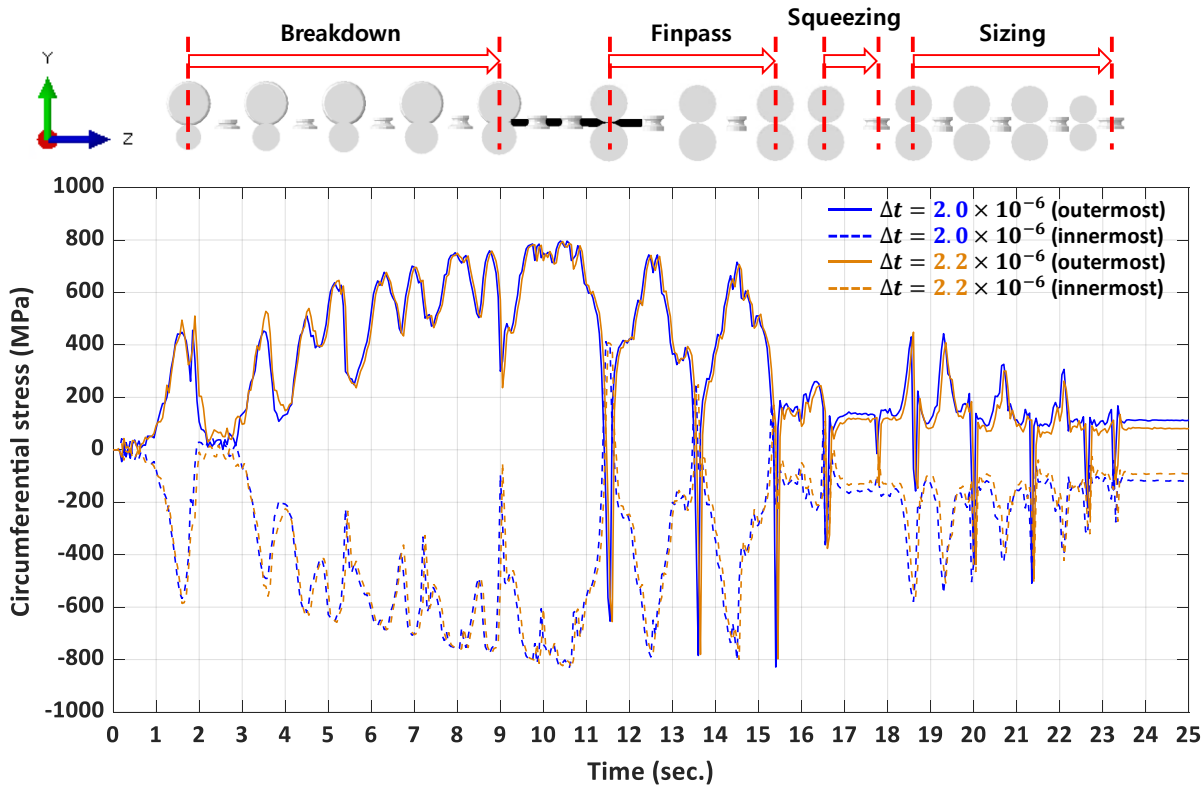

Fig. 2.7. Stress history during the manufacturing process at the opposite line of the seam weld:

$$\Delta t = 2.0 \times 10^{-6} \text{ vs } \Delta t = 2.2 \times 10^{-6}$$

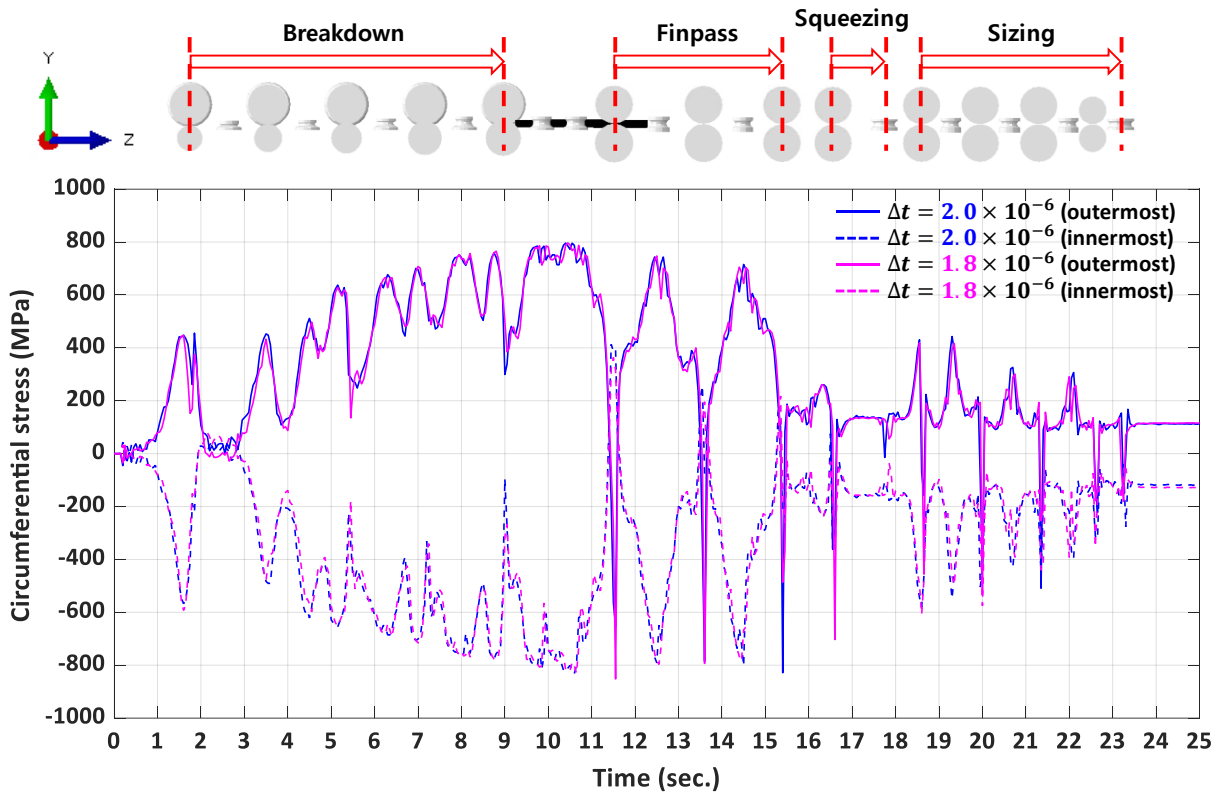

Fig. 2.8. Stress history during the manufacturing process at the opposite line of the seam weld:

$$\Delta t = 2.0 \times 10^{-6} \text{ vs } \Delta t = 1.8 \times 10^{-6}$$

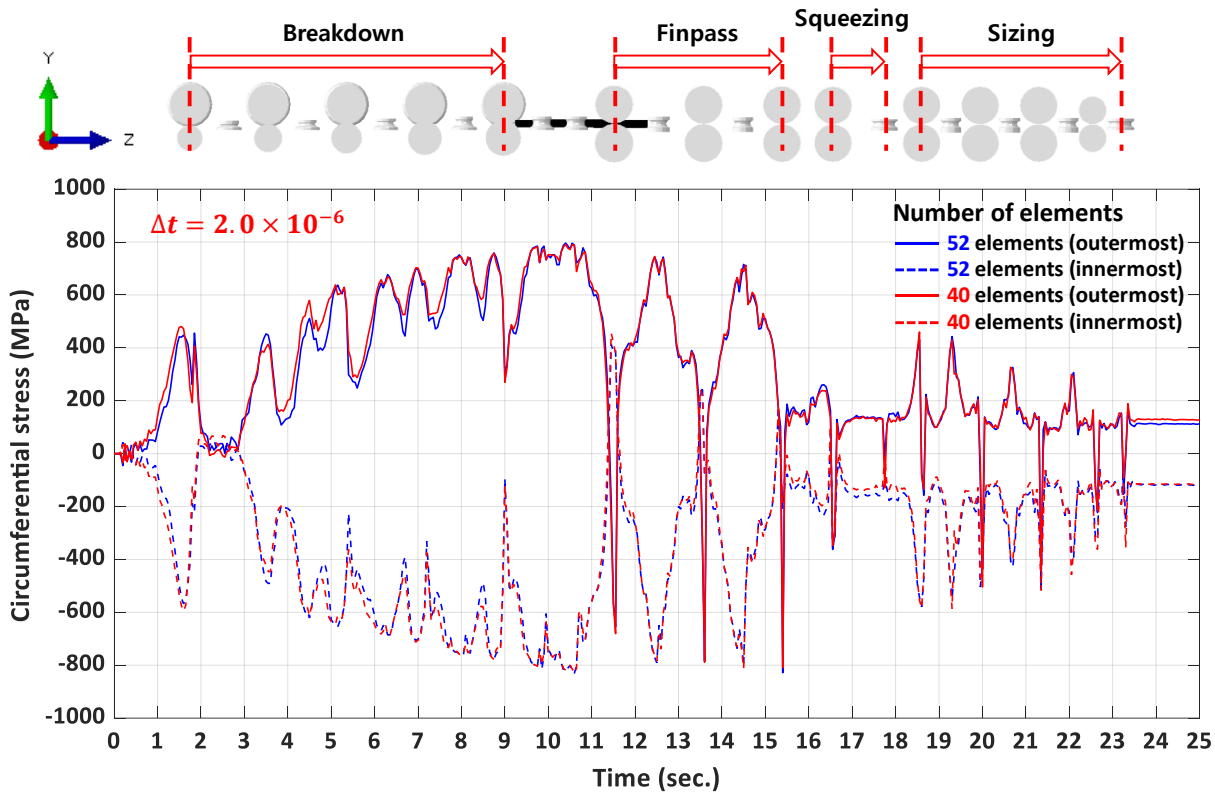

Fig. 2.9. Stress history during the manufacturing process according to mesh size in the transverse direction of the plate

2.4.2 Mesh size of the steel plate

As shown in Figs. 2.6-8, it has different stress history depending on the evaluation position in the thickness direction of the pipe. In other words, it is necessary to investigate how many elements must be constructed in the thickness direction of the pipe so that the analysis results converge. According to the simulation results of UOE steel pipe manufacturing process process by Yi (2017) and Kyriakides and Corona (2007), seven elements constructed along the thickness direction of the pipe are enough in simulation. So, in this study, seven elements were constructed along the thickness direction of the pipe.

The length of the plate was 7 times the width, and the plate was divided into 100 elements along the longitudinal direction of the pipe.

The main direction of deformation during the pipe manufacturing is the circumferential direction of the pipe, that is, the width direction of the plate. It is necessary to examine how many elements the plate is composed of in the transvers direction. If the plate width is divided into too few elements, the stiffness in the transverse direction becomes too large. On the contrary, if the plate width is divided too much, the analysis time is too long. As shown Fig. 2.9, the stress histories were compared when divided into 52 and 40 in the transverse direction. Even after the finpass, the difference between stress histories was insignificant, and the residual stress after the sizing was also

insignificant. In this study, the plate was divided into 52 elements in the transverse direction.

CHAPTER 3

QUALITY EVALUATION OF ERW PIPE CONSIDERING MANUFACTURING PROCESS

After the manufacturing, the pipe should have a certain level of quality. The typical example of the quality tests are out-of-roundess of cross-section, residual stress and yield strength. In Chapter 3, two adjustable conditions for the manufacturing process in practice based on the history of deformation were presented, and it was examined how the quality of ERW pipe changes according to the conditions of the manufacturing process.

3.1 Geometric characteristics of ERW pipe

The information that can be intuitively understood from the pipe is the geometric deformation before and after the manufacturing. In other words, the width and thickness of the plate before the manufacturing and the girth and thickness of the pipe after the manufacturing. It is necessary to understand the characteristics of the ERW pipe manufacturing process through this geometric information.

3.1.1 Deformation history during ERW pipe manufacturing process

As shown in Fig. 3.1, the plate undergoes the following history of deformation during the manufacturing. First, change in the width of the plate, which means the length of the neutral layer, is minimal until the breakdown due to free-bending. However, through the finpass process, the length of the neutral layer decreases as the welding surfaces contact the fins of the finpass rollers. In other words, while the compression acts in the circumferential direction, the length of the neutral layer is reduced. In order to keep the volume of the plate constant, the thickness and length are increased to compensate the reduced length of the neutral layer. In the sizing process, the compression in the circumferential direction as pipe was applied, and the thickness and length are increased like the finpass process.

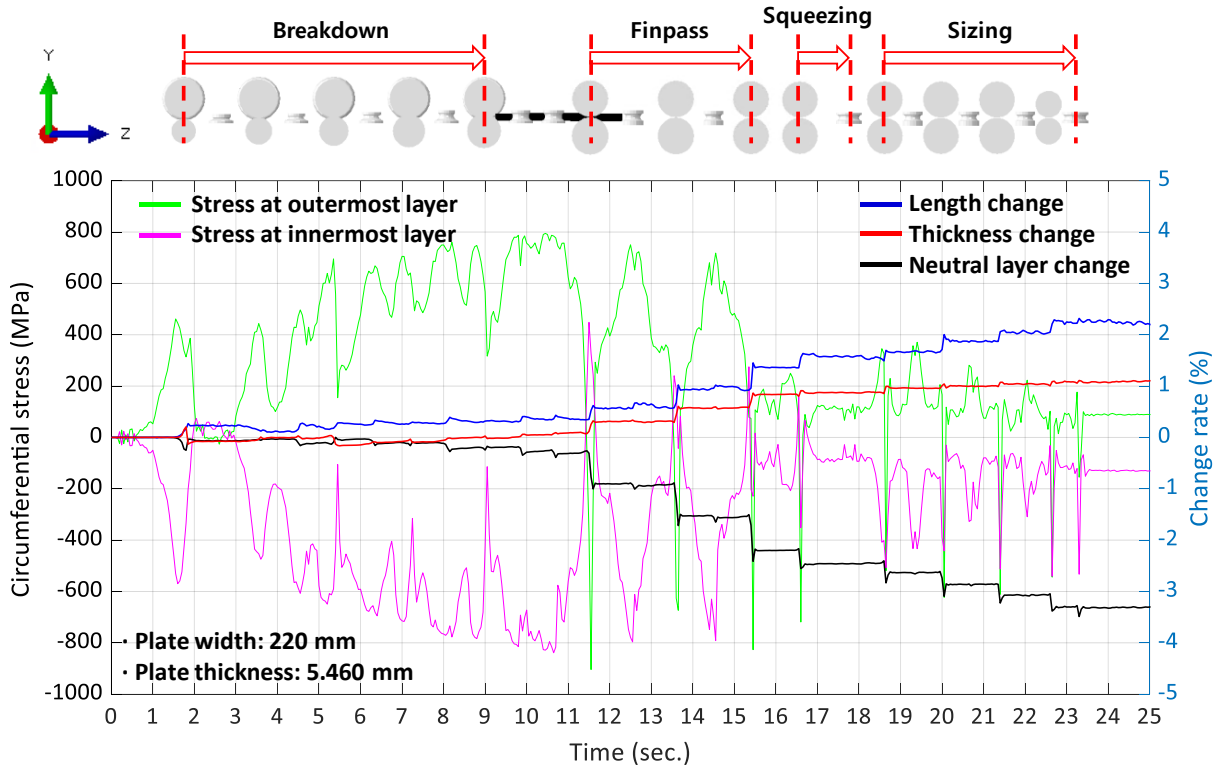

Fig. 3.1. Deformation history during the ERW pipe manufacturing process

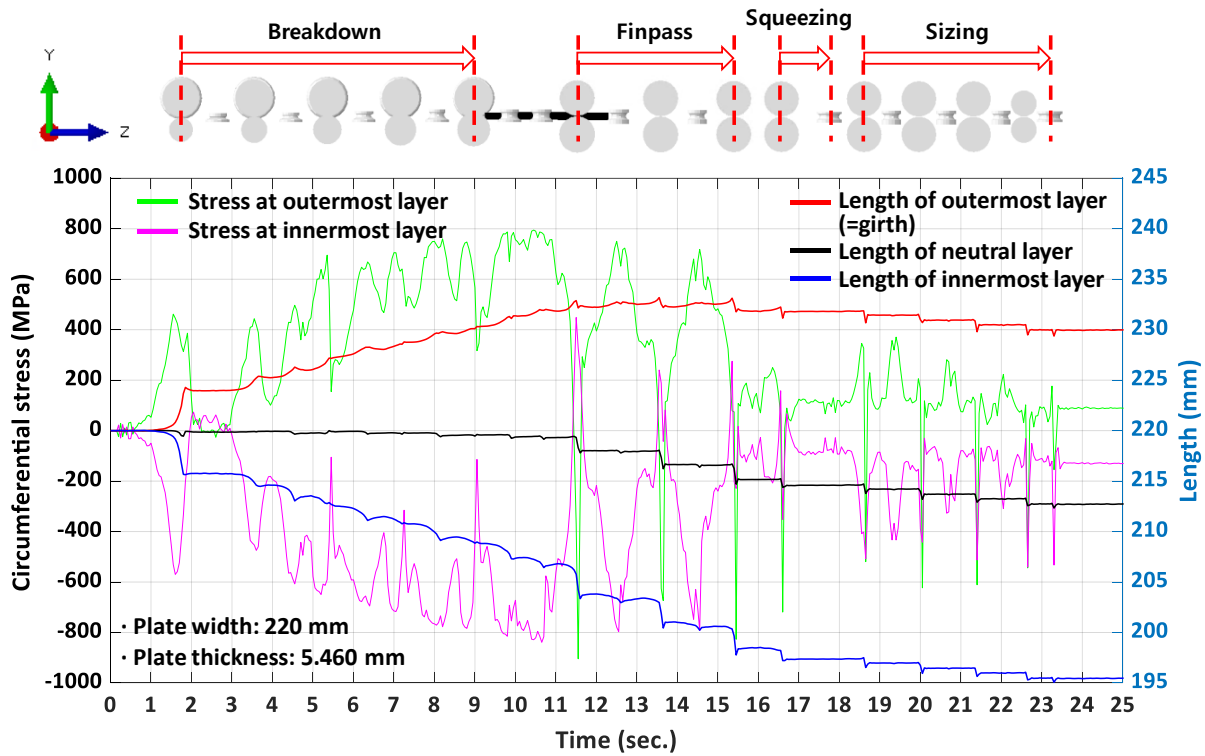

Fig. 3.2. Girth and length of neutral and innermost layers during the ERW pipe manufacturing process

Histories of the girth, length of the neutral layer and innermost layer during the manufacturing were evaluated as shown in Fig. 3.2. In the breakdown process, the change in the length of the neutral layer is insignificant, while the girth is increased and the length of the innermost layer is decreased by free-bending. It can be seen that a large compression is applied in the circumferential direction of the pipe when passing through the finpass and the sizing rollers.

In this study, the compression applied during the finpass and sizing processes were defined as roll-forming ratio and sizing ratio, respectively as Equations (3.1) and (3.2). As shown in Fig. 3.3, the roll-forming ratio is expressed as the reduced length of the neutral layer after passing the last finpass roller to the width of the steel plate. The sizing ratio means the rate of change of girth before and after the sizing process, and the girth decreases at a constant rate when it passes through four sizing roller sets same as the actual sizing method. In this study, the effect of the roll-forming and sizing ratios on the quality of the pipe was evaluated.

$$Roll\text{-}forming\ (RF)\ ratio = \frac{\Delta Neutral\ layer_{\ during\ roll\text{-}forming}}{Plate\ width} \quad (3.1)$$

$$Sizing\ (SZ)\ ratio = \frac{\Delta Girth_{\ during\ sizing}}{Girth_{\ before\ sizing}} \quad (3.2)$$

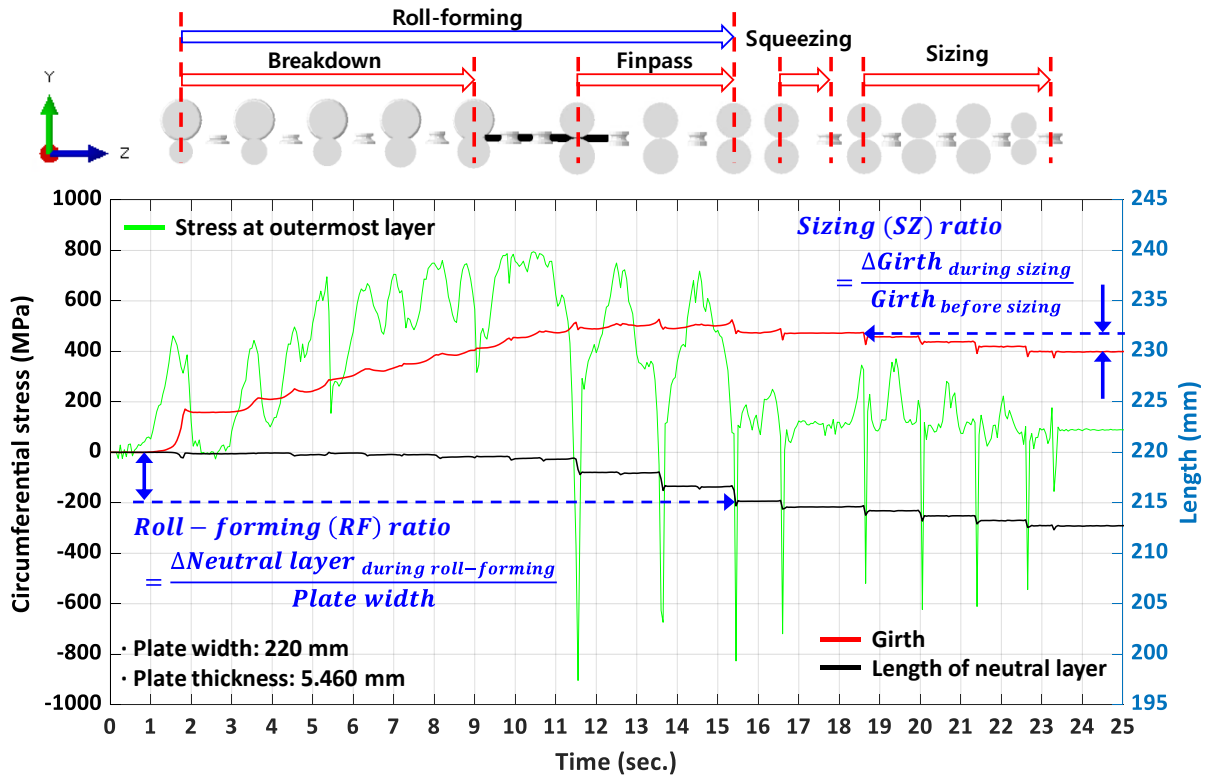

Fig. 3.3. Roll-forming and sizing ratios based on the girth and length of neutral layer

Table 3.1. Examples of girth history during the manufacturing

Manufacturing step		Measured girth (mm)						
		Case 1 (t=5.35 mm)	**Case 2 (t=9.15 mm)**	**Case 3 (t=9.07 mm)**	**Case 4 (t=9.5 mm)**	**Case 5 (t=12.3 mm)**	**Case 6 (t=10.65 mm)**	**Case 7 (t=15.6 mm)**
Sedan		219.0	542.0	548.0	591.0	666.0	688.0	835.0
Truck		232.0	565.0	571.0	-	-	-	882.0
After Finpass (FP)	**After FP1**	232.5	566.0	570.0	-	-	-	877.0
	After FP2	232.0	566.0	570.5	-	-	-	876.0
	After FP3	233.5	565.0	570.0	615.0	697.0	714.0	875.0
	RF ratio	0.98%	1.01%	1.13%	0.94%	1.08%	1.01%	1.02%
After squeezing		233.0	564.0	565.5	612.5	693.0	712.0	865.0
After sizing	**Girth**	231.0	560.0	562.0	609.0	689.0	707.0	860.0
	SZ ratio	0.86%	0.71%	0.62%	0.57%	0.58%	0.70%	0.56%

3.1.2 Design concept for rollers of roll-forming and sizing processes

The ERW pipe manufacturing process was designed using the previously defined the roll-forming and sizing ratios. Before that, the level of the roll-forming and sizing ratios in practice was investigated. In Table 3.1, the girth histories of the pipes were summarized for seven steel pipes of different sizes. In the breakdown process, the girth is increased relative to the width of the steel plate. In the finpass process, like the breakdown porcess, the bending occurs to match the target curvature, so the length of the girth should be increased gradually, but it was kept constant. The reason is that the plate is in contact with the fin of the finpass roller and the deformation in the circumferential direction is constrained. In seven cases, the roll-forming ratio was about 1% regardless of the diameter of the steel pipe.

On the other hand, unlike the roll-forming ratio, the sizing ratio was different according to the diameter of the steel pipe. One characteristic is that the larger the diameter of the steel pipe, the smaller the sizing ratio. In practice, the sizing ratio is generally applied at 0.2 to 1.0%. The rollers were designed as follows using information of the girth, the roll-forming and sizing ratios as shown in Fig. 3.4.

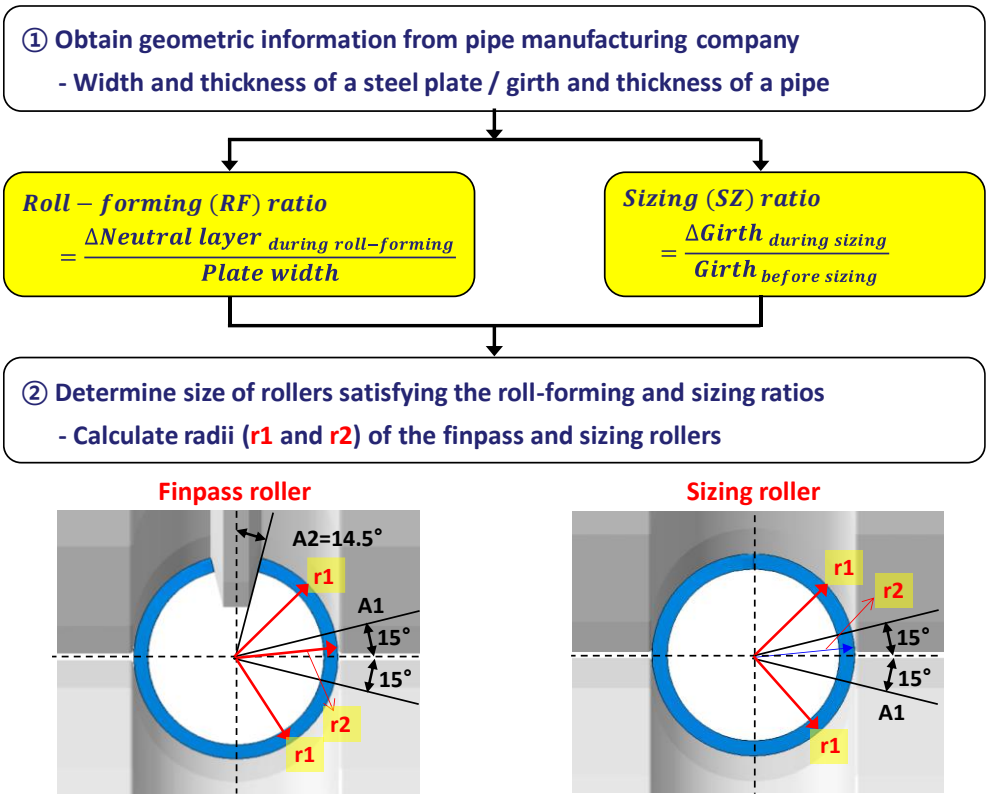

Fig. 3.4. Design concept of rollers from geometric information

Step 1: Once the target roll-forming ratio is determined, the length of the neutral layer is calculated by considering the width and thickness of the plate that meets the target roll-forming ratio.

Step 2: Determine the size of the last finpass roller through which the plate with the target neutral layer length can pass. Here, the shape of the finpass roller is determined by decreasing or increasing the radii which is one of parameters composing the shape of the finpass roller.

Step 3: Determine the shape of the first and second finpass rollers which make the pipe pass with the target length of the neutral layer calculated in the step1. The size of the rollers is also determined by adjusting the radii.

Step 4: The shape of the squeezing roller is determined by adjusting the radii so that the girth after passing the finpass does not change.

Step 5: Once the target sizing ratio is determined, the amount of girth reduction during the sizing process is determined. That is, the shape of each sizing roller is determined such that it can be reduced by a quarter of the target girth reduction amount while passing through each of the four sizing rollers. The size of the rollers is also determined by adjusting the radii.

3.1.3 Dependency of ovality on roll-forming and sizing ratios

One of the important quality evaluation factors of steel pipes is the out-of-roundness of cross-section which affects the structural performance of steel pipes. In the practice, through measurement of diameter as shown in Fig. 3.5a, the out-of-roundenss defined as ovality is calculated as Equation (3.3). DNV-OS-F101, which is the offshore pipeline design standard, proposes a maximum allowable ovality of 3%. However, in this study, it is difficult to calculate the exact diameter after the manufacturing using the coordinates of the nodes. Therefore, as shown in Fig. 3.5b, the center of the cross-section was calculated by using the coordinates of each node, and then the radii from the center were obtained to calculate the ovality as Equation (3.4).

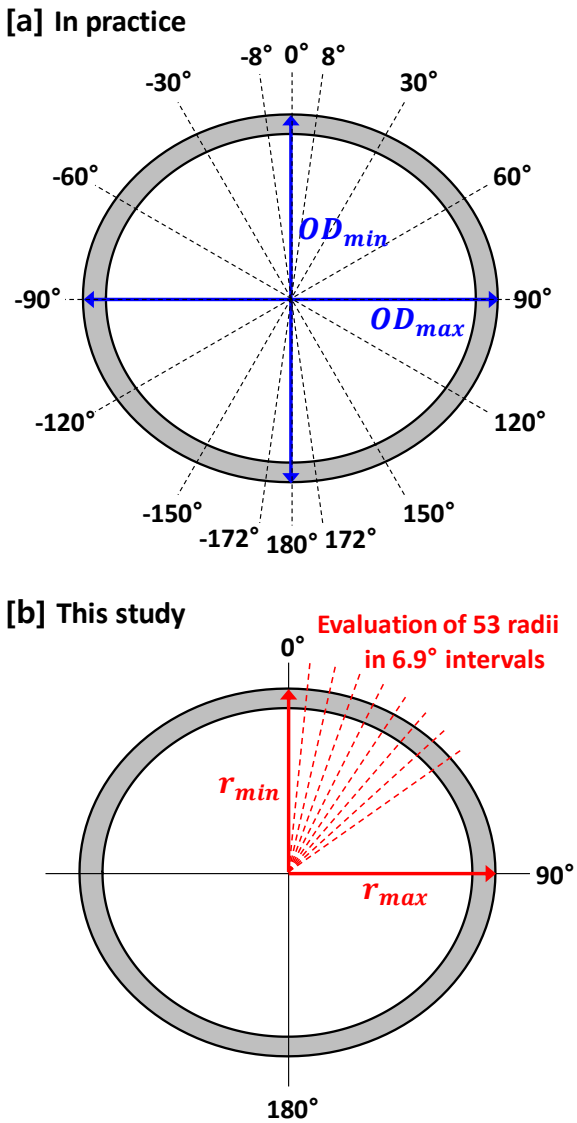

Fig. 3.5. Measurement of diameter for evaluating the ovality: (a) in practice, and (b) in this study

$$Ovality_1 = \frac{OD_{max} - OD_{min}}{OD_{avg}} \tag{3.3}$$

$$Ovality_2 = \frac{r_{max} - r_{min}}{r_{avg}} \tag{3.4}$$

As in previous studies, one of the roles of the sizing process is to improve the ovality. As shown in Fig 3.6, varation of ovality according to the roll-forming and sizing ratios. The smaller the roll-forming ratio, the greater the ovality before the sizing, but the ovality was improved to a similar level through the sizing. In addition, the improvement of ovality was similar at sizing ratio of more than 0.5%, and the ovality was improved up to 0.4-0.5% by the sizing.

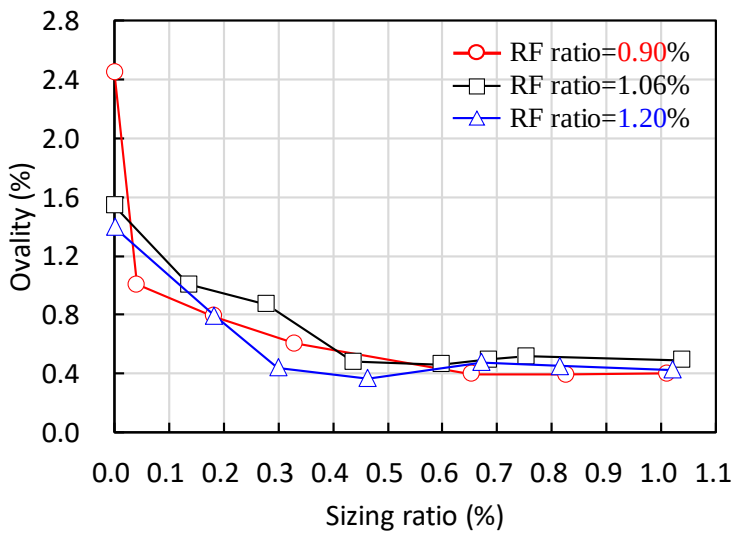

Fig. 3.6. Dependency of ovality on roll-forming and sizing ratios

3.2 Residual stress after the ERW pipe manufacturing process

The presence or absence of residual stress in the pipe after the manufacturing is also an important factor on the structural performance of the pipe. In this section, the effects of the roll-forming and sizing ratios on residual stress were evaluated.

3.2.1 Stress history of each layer at opposite line of the seam weld

The stress history during the manufacturing is different according to evaluation positions. The stress history at the opposite line of the seam weld with the least effect of the welding process was investigated. As shown in Fig. 3.2, cycling of the stress caused by the springback that occurs immediately after passing the rollers continues through the breakdown process. In addition, during the finpass process, compression occurs in the outermost layer while tension occurs in the innermost layer. In other words, until the finpass process, the opposite stress histories are observed in the innermost and outermost layers. In the sizing process, the compression is applied on both innermost and outermost layers through four roller sets. According to the previous studies by Han et al. (2019) and Nishimura et al. (1997), one of the roles of the sizing is to reduce the amount of residual stress after roll-forming. As a result, the overall residual stress after the finapss was reduced, and the residual stresses of tension and compression occurred in the outermost and innermost layers, respectively after the sizing.

3.2.2 Dependency of residual stress on roll-forming and sizing ratios

In Fig. 3.7, it is evaluated how the residual stress decreases according to the sizing ratio. The residual stresses were evaluated at the outermost and innermost layers of the opposite line of the seam weld. Depending on the

sizing ratio, the difference in residual stress after the sizing was small. The residual stress after the manufacturing was about 15% of the yield strength of the steel plate.

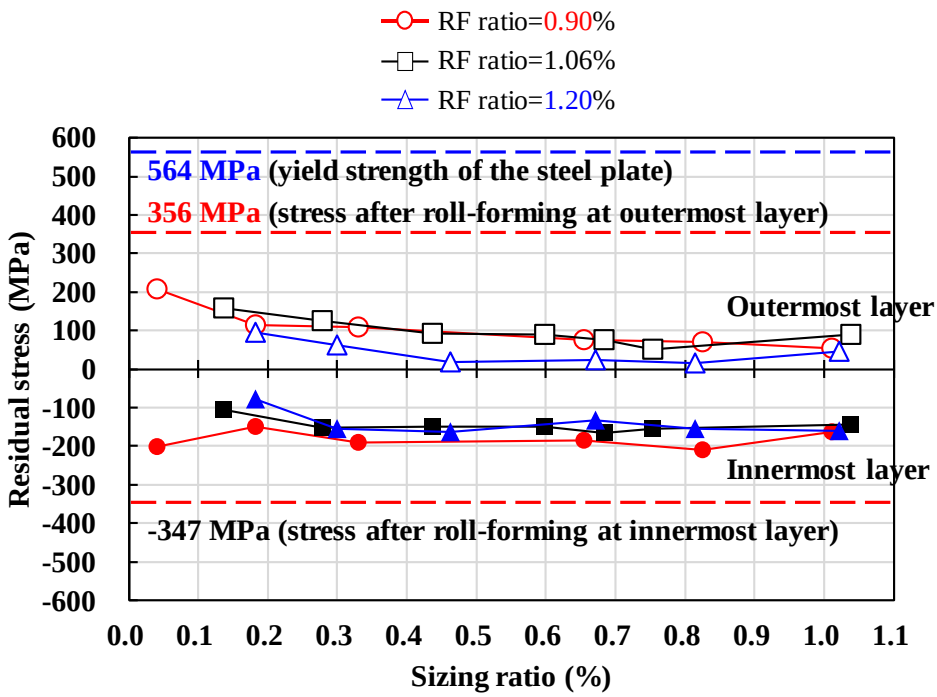

Fig. 3.7. Dependency of residual stress on roll-forming and sizing ratios

3.3 Prediction of yield strength after manufacturing for quality control

As one of the quality tests, the pipe has to achieve the target yield strength after the manufacturing. However, plastic deformation in the manufacturing changes the stress-strain relationship of the plate due to the strain hardening

and the Bauschinger effect, which leads to a decrease or increase in yield strength. In addition, since the deformation history is also different in the thickness direction, the yield strength after the manufacturing has variation depending on the evaluation position. In this section, it is evaluated how the tensile and compressive yield strengths changed by manufacturing.

3.3.1 Simulation of flattening process for tensile test

Since the specimens extracted from the pipe after manufacturing are bent, the flattening process is required to make the tensile test specimen. However, plastic deformation occurring in the flattening process also affects change in the yield strength.

According to previous study (Rashid et al., 2018), there are a variety of flattening methods. The flattening method is different for each company and there is no standardized method. In this study, four-point bending method was adopted.

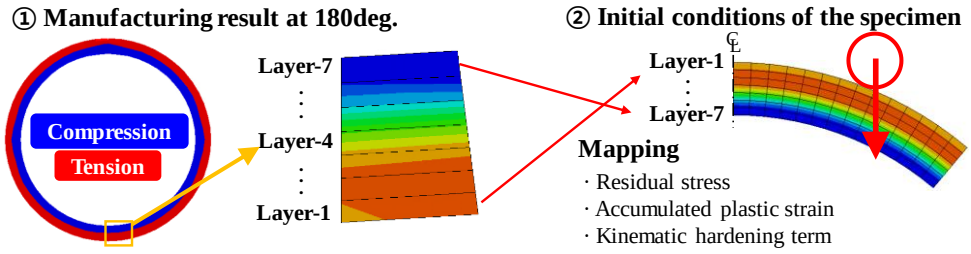

Fig. 3.8. Mapping for the flattening analysis

The mapping is used to maintain the continuity between the manufacturing analysis and the flattening analysis. As shown in Fig. 3.8, the kinematic hardening term, accumulated plastic strain and residual stress at opposite line of the seam weld were assumed as initial inputs of the flattening model, so that modified stress-strain relationship can be considered. In addition, the flattening specimens were also composed of seven layers along the thickness direction in order to consider different deformation histories. The shape of the flattening specimen was the same as the thickness and curvature of the pipe, and was flattened by compressing it at the top as shown in Fig. 3.8. Tension and compression occurred in the innermost and outermost layers during the flattening, and the springback of the specimen was simulated after the flattening.

3.3.1 Simulation of tensile and compression tests

For continuity between the flattening and tensile test analysis, the mapping method used in the flattening analysis was also used. Kinematic hardening term, accumulated plastic strain and residual stress in each layer after the flattening were set as initial input of the tensile test specimen. The specimen for the tensile test were also composed of seven specimens in the thickness direction to take account for the different deformation history in the thickness direction. As shown in Fig. 3.9a, the tensile test specimen is dog-bone shape

according to ASTM, and the thickness of the specimen was set equal to the that of the pipe.

(a) Tensile test **(b) Compression test**

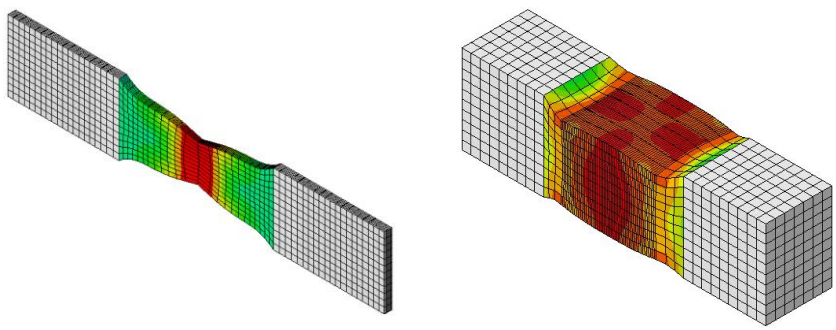

Fig. 3.9. Specimen for (a) tensile test, and (b) compression test

The compression test was conducted without the flattening process. That is, the kinematic hardening term, accumulated plastic strain, and residual stress at opposite line of the seam weld after manufacturing were mapped to the specimen for the compression test. The shape of the specimens was also modeled according to ASTM as shown in Fig. 3.9b.

3.3.2 Yield strength in the circumferential direction of pipe

Tensile stress-strain relationship o before and after the flattening is shown in Fig. 3.10. Yield plateau disappeared by repetitive loading-unloading-reloading during the manufacturing, and the Bauschinger effect is shown by compression applied during the finpass and sizing process. Due to the flattening, the stress-strain relationship is increased.

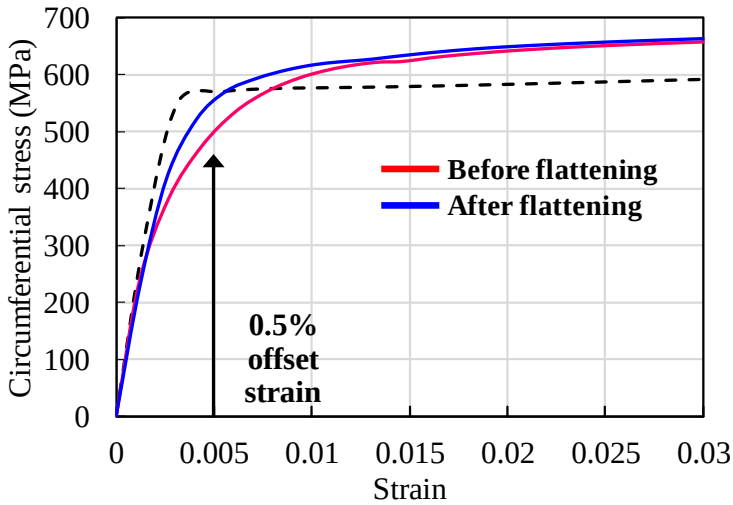

Fig. 3.10. Stress-strain relationship by tensile test

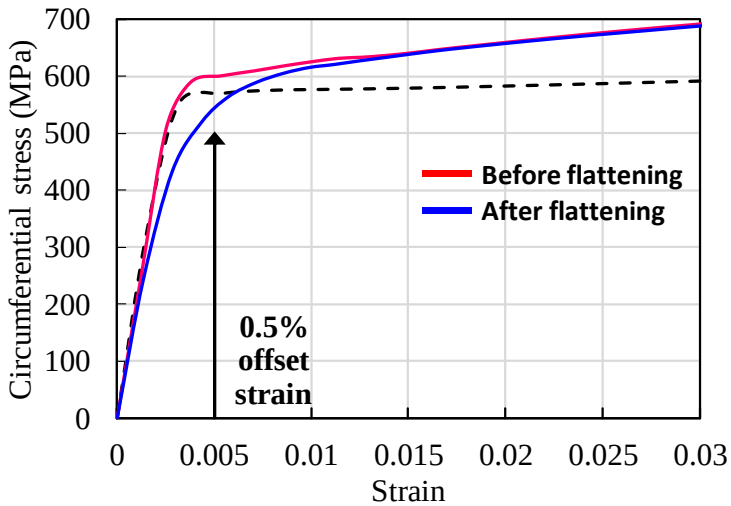

Fig. 3.11. Stress-strain relationship by compression test

Table 3.2. Yield strength after ERW pipe manufacturing

	Tensile YS (MPa)	**Compressive YS (MPa)**
Steel plate	567	567
Before flattening	497 (-12%)	597 (5%)
After flattening	551 (-3%)	559 (-1%)

As shown in Table 3.2, the tensile yield strength evaluated at 0.5% offset strain according to API was 497 MPa before the flattening and was 551 MPa after the flattening, which was 12% and 3% less than that of the steel plate, respectively.

On the other hand, as shown in Fig. 3.11, the compressive stress-strain relationship before the flattening shifted upward by the strain hardening. It leaded that the compressive yield strength at 0.5% offset strain increased to 597 MPa, which was 5% higher than that of the steel plate. In order to examine the effect of the flattening, the compressive yield strength after flattening was also evaluated. After the flattening, the Bauschinger effect was observed and the compressive yield strength was reduced to 559 MPa.

3.3.4 Yield strength according to sizing ratio

The effects of the roll-forming and sizing ratios on the yield strength are evaluated as shown in Fig. 3.12. There was no difference in the yield strength depending on the roll-forming ratio. However, as the sizing ratio increased,

the compressive and tensile yield strength gradually increased and decreased, respectively. This is because the circumferential compression increases as the sizing ratio increases, so the effects of the strain hardening and the Bauschinger effect on the stress-strain relationship increase. The effect of sizing ratio was greater on the compressive yield strength than on the tensile yield strength.

Tensile yield strength after flattening did not show any difference according to sizing ratio. After flattening, tensile yield strength decreased about 4% compared to that of the steel plate.

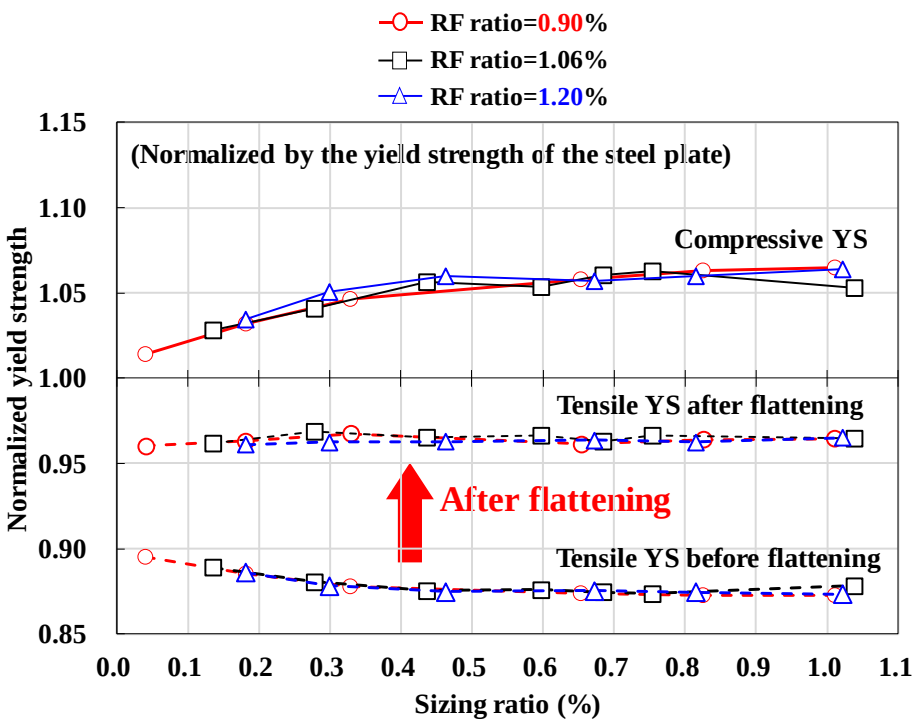

Fig. 3.12. Dependency of yield strength on roll-forming and sizing ratios

CHAPTER 4

COLLAPSE ANALYSIS OF ERW PIPE CONSIDERING MANUFACTURING PROCESS

4.1 Collapse analysis considering ERW pipe manufacturing

4.1.1 Definition of the collapse

Collapse phenomena of the pipe have been the subject of a great deal from the 1980's up to now. According to a design code for offshore pipeline (DNV-OSF101), collapse is a kind of local buckling in which gross deformation of the cross section confined to a short length of the pipe occurs. When the local buckling is triggered only by external over pressure, corresponding limit state is defined as collapse. Collapse of the pipe can be treated as a local buckling behavior of column structure.

The response of the API X70 (Yield strength = 521 MPa) pipe under external pressure is shown in Fig. 4.1, where P and P_0 are uniform external pressure and yield pressure, respectively. Horizontal axis indicates the maximum radial deflection of the pipe normalized by outer radius. At a certain critical pressure followed by linearly increasing pressure, perfect pipe bifurcates into a fundamental buckling mode of uniform-ovality shape. Buckling usually takes place in plastic region beyond elastic limit for this kind of thick pipes, so that it referred to as plastic buckling. Through a

bifurcation point, the pressure increases monotonically to maximum value, which is defined as a collapse pressure. After reaching the collapse pressure, the response follows decreasing trajectory as collapse gets localized. In other words, the pipe becomes useless structurally over collapse pressure.

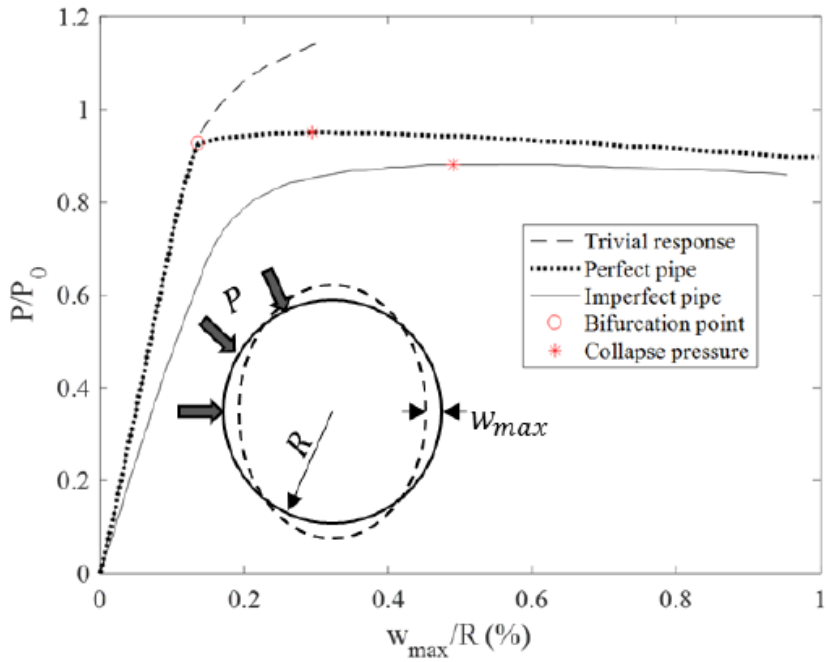

Fig. 4.1. Nonlinear external pressure-maximum displacement response of the pipe

4.1.2 Initial conditions of collapse analysis

The pipe model of the collapse analysis was adopted from that of the manufacturing analysis to reflect the manufacturing results. That is, the modified stress-strain relationship, the configuration of the pipe such as the ovality and distribution of residual stress after the manufacturing was

reflected. And then, the new boundary conditions eliminating the original boundary conditions for the manufacturing analysis were added. As shown in Fig. 4.2, the length of the pipe was about 22 times the diameter, and both ends were fixed in all directions, and the pipe was subjected to uniform external pressure. The length of the zone subjected to uniform external pressure was 14 times the diameter, and according to Yi (2017), the effect of the boundary conditions at both ends can be ignored at the center when the length the zone b is more than 10 times the diameter. For nonlinear analysis, the collapse pressure was evaluated using the modified Riks method.

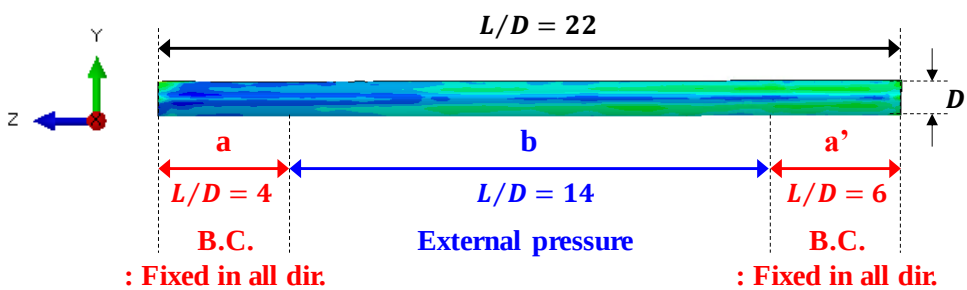

Fig. 4.2. Boundary conditions for collapse analysis

4.1.3 Mechanism of collapse under external pressure

The mechanism of collapse under external pressure was investigated through the change of stress distribution in the circumferential direction of the pipe. As shown in Fig. 4.3, first, the stress distribution was checked as it passed through the sizing process in order to examined how the stress distribution of the ERW pipe was generated. Compression was applied in the circumferential direction while passing through the sizing rollers, with compression concentrated at the inner layers of 45 degrees, 135 degrees, 225 degrees and 315 degrees due to shape of the rollers. At the end of the manufacturing after the sizing, the stress was concentrated at 180 degrees (i.e. the opposite line of the seam weld). This is because the compressive stress concentrated at 135 degrees and 225 degrees after the sizing compresses the inner layer of 180 degrees due to the stress redistribution caused by self-equilibrium. That is, after the ERW pipe manufacturing process is completed, residual stresses of compression and tension are concentrated in the inner and outer layers at 180 degrees, respectively.

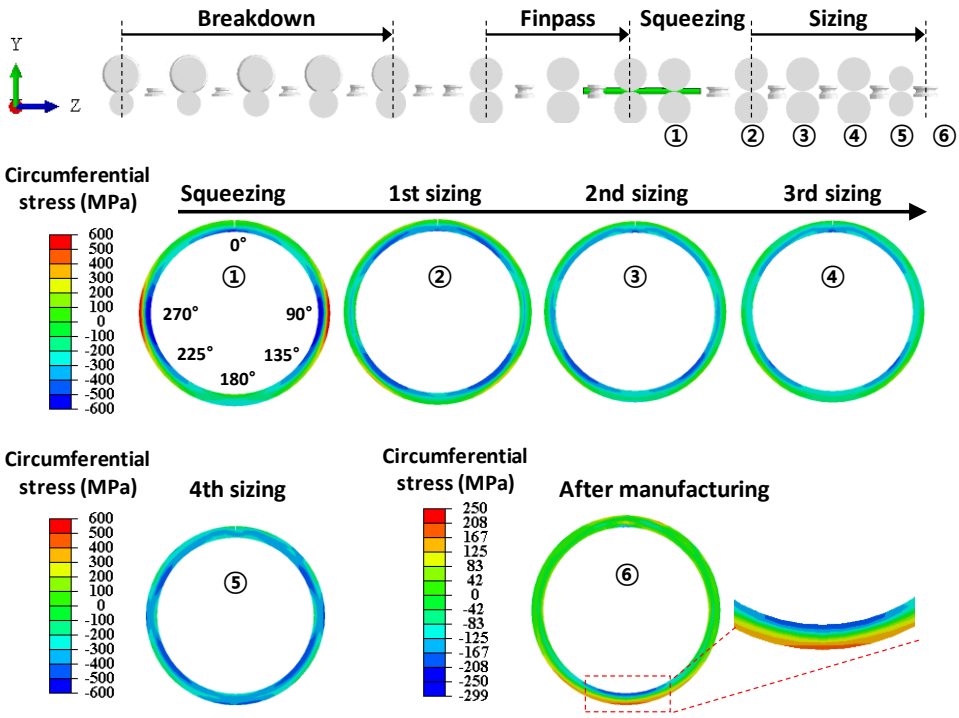

Fig. 4.3. Stress distribution during the sizing process

The distribution of the stress in the circumferential direction was investigated under external pressure considering ERW pipe manufacturing process. As shown in Fig. 4.4, the circumferential stress distribution and the relationship between displacement and external pressure were investigated together. As the external load was applied, the compressive stress began to concentrate at 180 degrees where the stress was concentrated after the ERW pipe manufacturing process. When the maximum external pressure was applied, local buckling occurred in the inner layer of 180 degrees. Then, the displacement increased rapidly even though the external pressure decreased due to reduced stiffness of the ERW pipe. After the local buckling occurred, the cross section became ellipse.

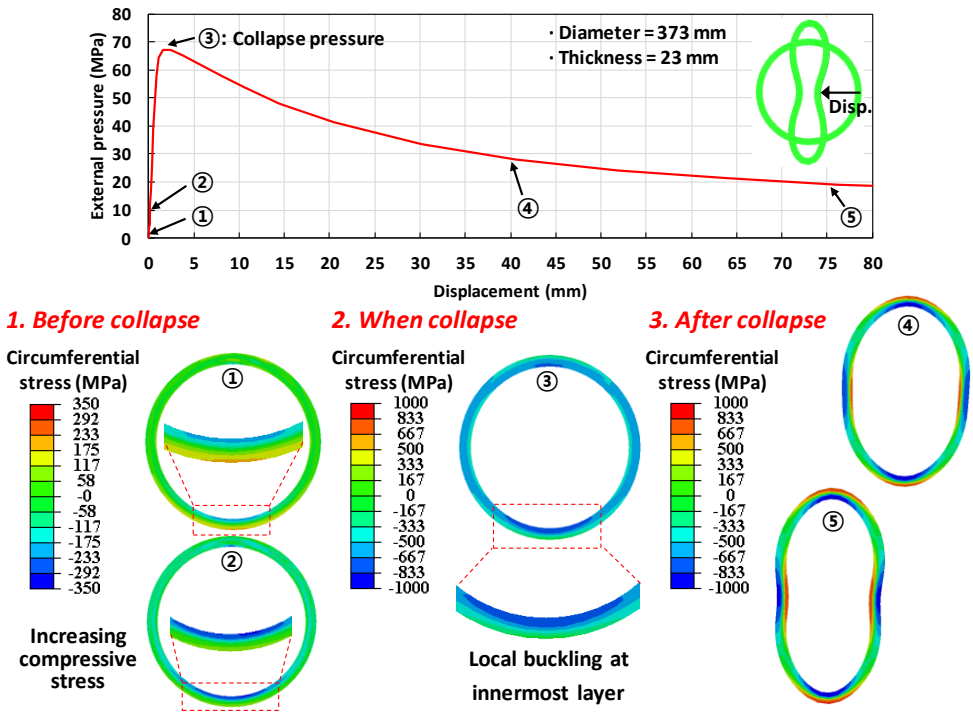

Fig. 4.4. Stress distribution under external pressure

4.2 Influence factors on collapse performance

4.2.1 Effect of initial ovality

Geometric imperfection is a critical factor in deteriorating the structural performance of steel pipes. As shown in Fig. 4.5, the collapse pressure is greatly reduced by the existence of the ovality. At 0.5% of ovaltiy, which is general value of ERW pipe in practice, collapse pressure was reduced by about 30 to 40% compared to that of a pipe without ovality. As the ovality increases, the collapse pressure gradually decreases, but the effect of ovality

on the collapse pressure decreases gradually. As the ovality increases from 0.6 to 1%, the collapse pressure decreases by about 5%.

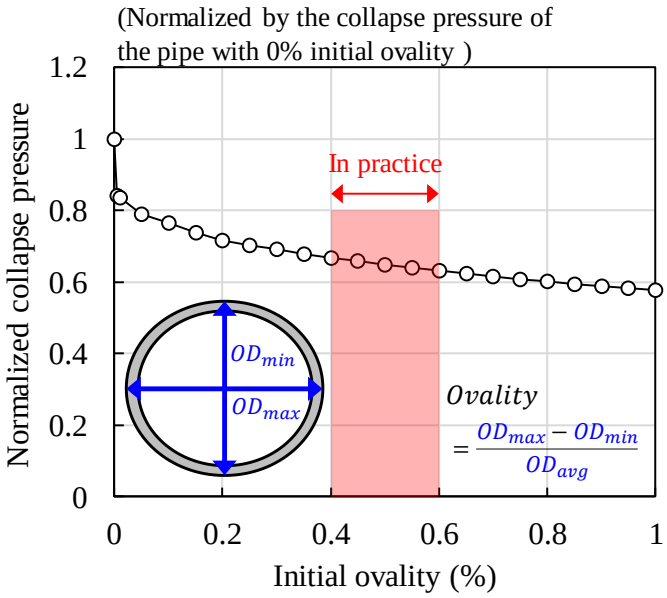

Fig. 4.5. Effect of initial ovality on collapse analysis

4.2.2 Effect of residual stress

The shape of the cross-section and the circumferential stress distribution at the moment when collapse occurs are shown in Fig. 4.6. When the collapse begins to occur, the innermost layer on the side with the largest diameter initiates to yielding. Therefore, the residual stress of the innermost layer is an important factor in the collapse pressure evaluation. Following results for circumferential residual stress is evaluated at the innermost layer.

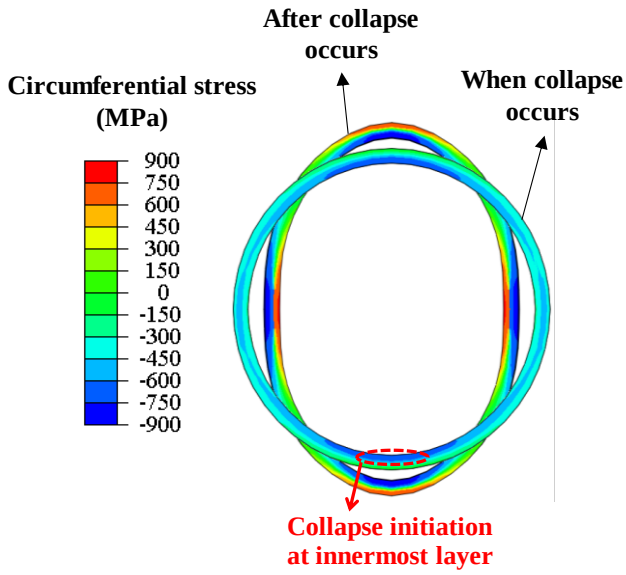

Fig. 4.6. Shape of a cross-section when collapse occurs

4.2.3 Effect of seam welding

To assess the structural performance of steel pipes, welds are always considered a weak point. Since the welding method varies depending on the type of steel pipes, it is necessary to understand the effect of ERW welding. However, due to the characteristics of the continuous manufacturing process of ERW pipes, it is difficult to track and evaluate the characteristics of electric resistance welding process. The measured residual stresses of steel pipes and the characteristics of residual stress generated by welding were investigated instead from the previous studies.

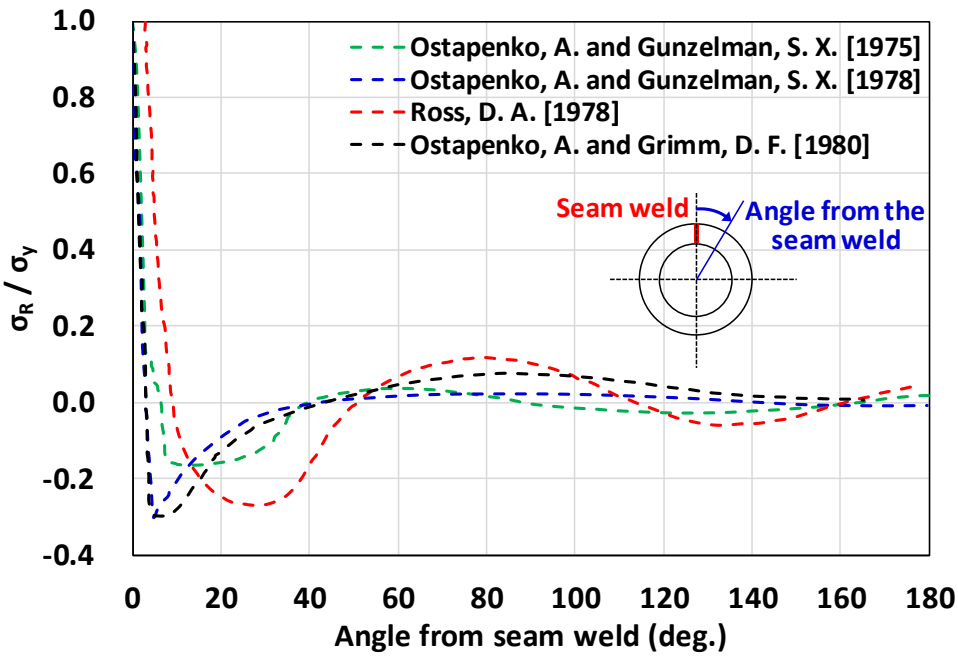

Fig. 4.7. Measured residual stress of pipes in the previous studies for axial compression tests

As shown in Fig. 4.7, the residual stress in the longitudinal direction of the steel pipes for the axial compression test were measured (Ostapenko and Gunzelman, 1975; Ostapenko and Gunzelman, 1978; Ross, 1978; Ostapenko and Grimm, 1980). In the seam weld, the tensile residual stress as much as the yield strength were generated, and the magnitude of residual stress rapidly decreased as going farther from the seam weld. On the opposite side of the seam weld, the effect of welding on the residual stress was minor. Chen and Ross (1978), on the other hand, evaluated the residual stress in the circumferential direction of the pipe. The circumferential residual stress at the opposite side of the seam weld was mainly generated by physical bending during forming, and the effect of the seam welding was minor.

Roy (2006) examined the characteristics of residual stress distribution in the thickness direction after fillet welding. Like the result in Fig. 4.7, tensile residual stress occurred in the outer layer where the fillet welding was performed. And then, the residual stress decreases rapidly as going farther from the seam weld. That is, where the welding is performed, great tensile residual stress is generated by the heat generated during welding, and the magnitude of the residual stress decreases rapidly as the distance from the weld is increased.

The results of previous studies were applied to the ERW pipe. During the welding process of the ERW pipe, both heated weld surfaces are bonded by only physical external pressure. This means that because the welding surfaces are attached at the same time in the inner and outer layers, residual stresses due to the welding will occur symmetrically about the neutral axis leading to tensile residual stress in the inner layer. In addition, in the ERW process, the seam annealing is essentially carried out to remove residual stress generated by seam welding. Considering the mechanism of the collapse caused by external pressure, the tensile residual stress caused by welding will have little effect on the ERW pipes.

4.3 Enhancement of collapse pressure by sizing process

As sizing reduces residual stress and improves ovality, collapse pressure will increase. The effects of ovality and residual stress by the ERW pipe manufacturing process on collapse pressure are evaluated to understand clearly the effect of sizing process.

4.3.1 Effectiveness of sizing process on collapse pressure

The collapse pressures before and after the sizing process are compared as shown in Fig. 4.8. The sizing process makes residual stress reduced and ovality improved, causing the collapse pressure to double. In Fig. 4.9, the effects of ovality and residual stress after the roll-forming process on collapse pressure were evaluated separately. In the presence of residual stress only, the impact on collapse pressure was small, while the ovality after roll-forming was fatal for reducing collapse pressure. In the presence of residual stress only, the impact on collapse pressure was small, while the ovality after roll-forming was fatal for reducing collapse pressure. In the presence of both ovality and residual stress, collapse pressure decreased most. Therefore, it is more effective to improve collapse pressure by improving ovality rather than reducing residual stress through the sizing process.

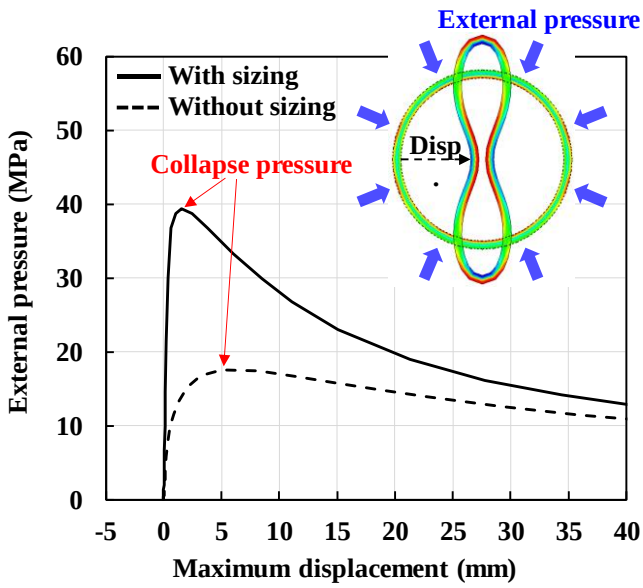

Fig. 4.8. Effect of the sizing process on enhancement of collapse pressure

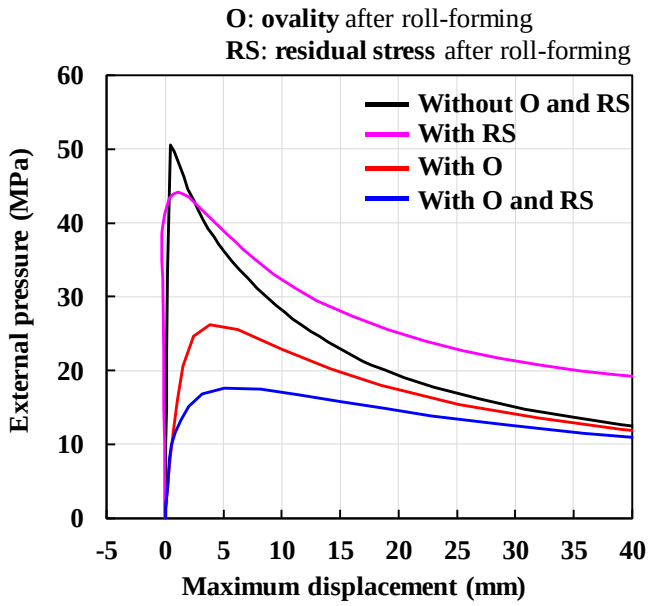

Fig. 4.9. Reduction in collapse pressure due to ovality and residual stress after the roll-forming

4.3.2 Collapse pressure according to roll-forming and sizing ratios

The ovality and collapse pressure were compared together according to the sizing ratio as shown in Fig. 4.10. As the sizing ratio increased, the ovality is improved, while the collapse pressure increased. In particular, at sizing ratios above 0.5%, the collapse pressure gradually increased despite improvement in ovality is minor. On the other hand, the collapse pressure dramatically increased under the sizing ratio of less than 0.4% due to improvement of ovality.

The residual stress and collapse pressure were compared together according to the sizing ratio as shown in Fig. 4.10. Although residual stress affects collapse performance, the effect of the sizing ratio on collapse pressure is negligible because there is no difference in residual stress after the sizing process.

The compressive yield strength and collapse pressure were compared together according to the sizing ratio as shown in Fig. 4.12. Compressive yield strength continued to increase with increasing sizing ratio, similar to variation of collapse pressure according to the sizing ratio. That is, when the sizing ratio was less than 0.4%, the collapse pressure increased due to the improvement of ovality, and at the sizing ratio above 0.4%, the collapse pressure increased with the increasing compressive yield strength.

In Fig. 4.13, the effect of the roll-forming and sizing ratios on the collapse pressure is evaluated. Collapse pressure tended to increase with increasing

sizing ratio regardless of roll-forming ratio, and collapse pressure increased up to 10% by the sizing process. Since the roll-forming ratio has a negligible effect on collapse pressure, collapse pressure is evaluated by sum of the roll-forming and sizing ratios as shown in Fig. 4.14. Collapse pressure of ERW pipe is greatly influenced by ovality and compressive yield strength generated by the manufacturing, which can be improved by sizing process.

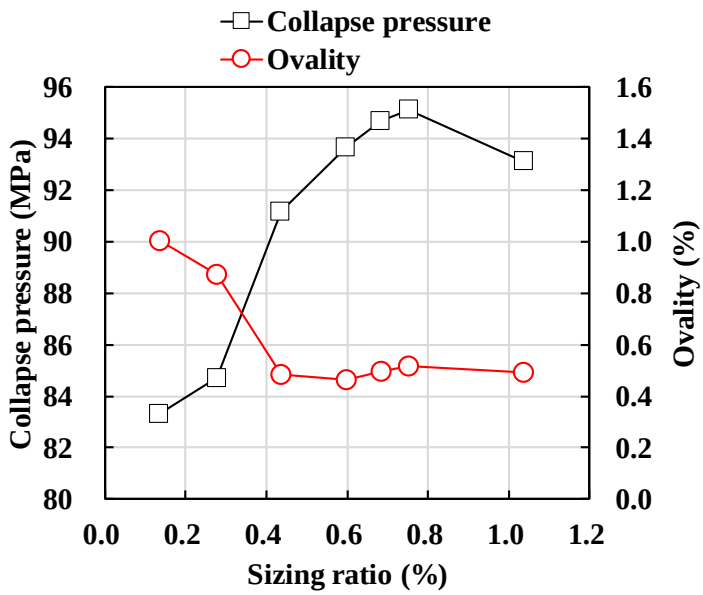

Fig. 4.10. Reduction in collapse pressure due to ovality and residual stress after the roll-forming

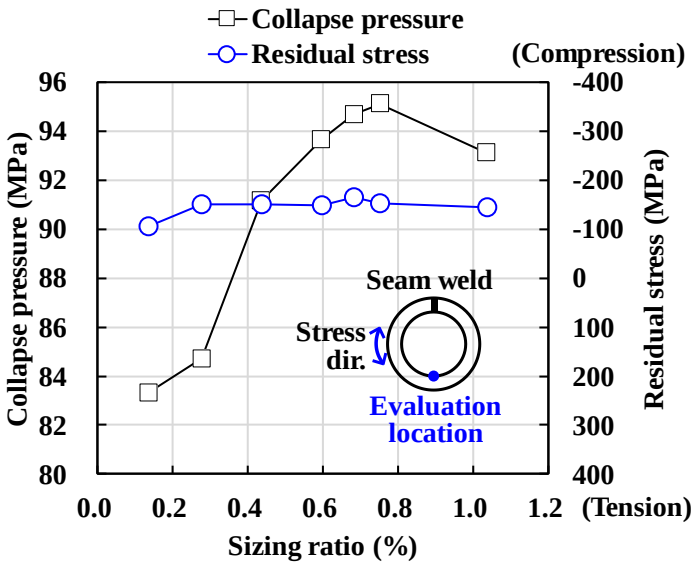

Fig. 4.11. Reduction in collapse pressure due to ovality and residual stress after the roll-forming

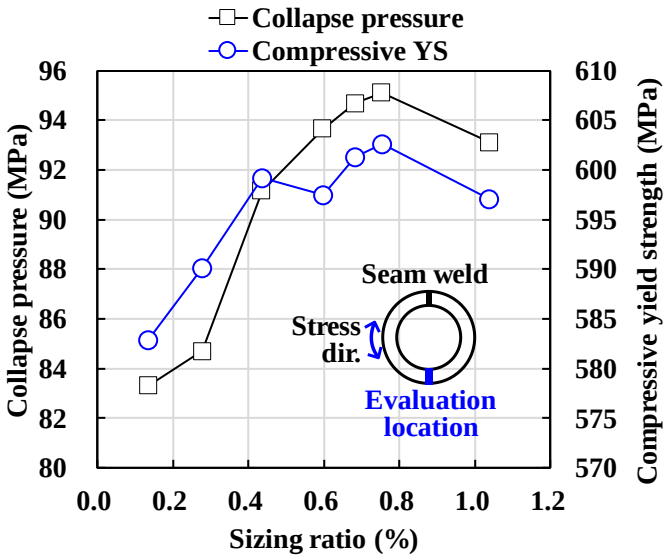

Fig. 4.12. Reduction in collapse pressure due to ovality and residual stress after the roll-forming

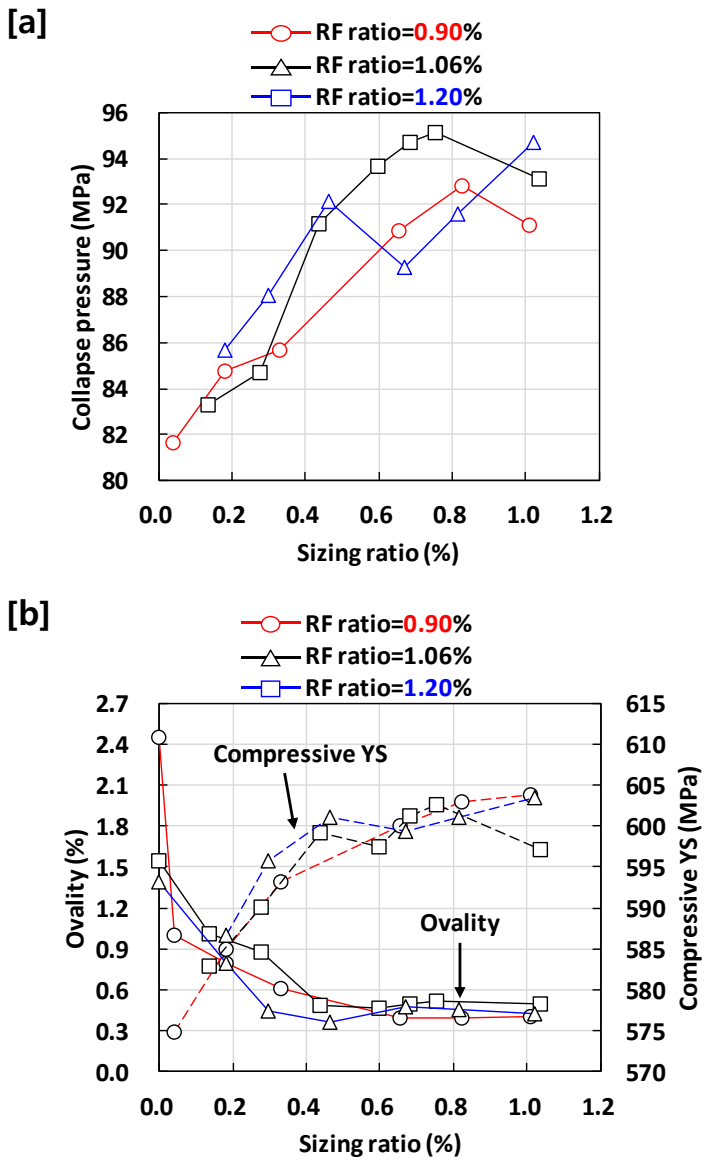

Fig. 4.13. Dependency of roll-forming and sizing ratios on (a) collapse pressure, and (b) ovality and compressive yield strength

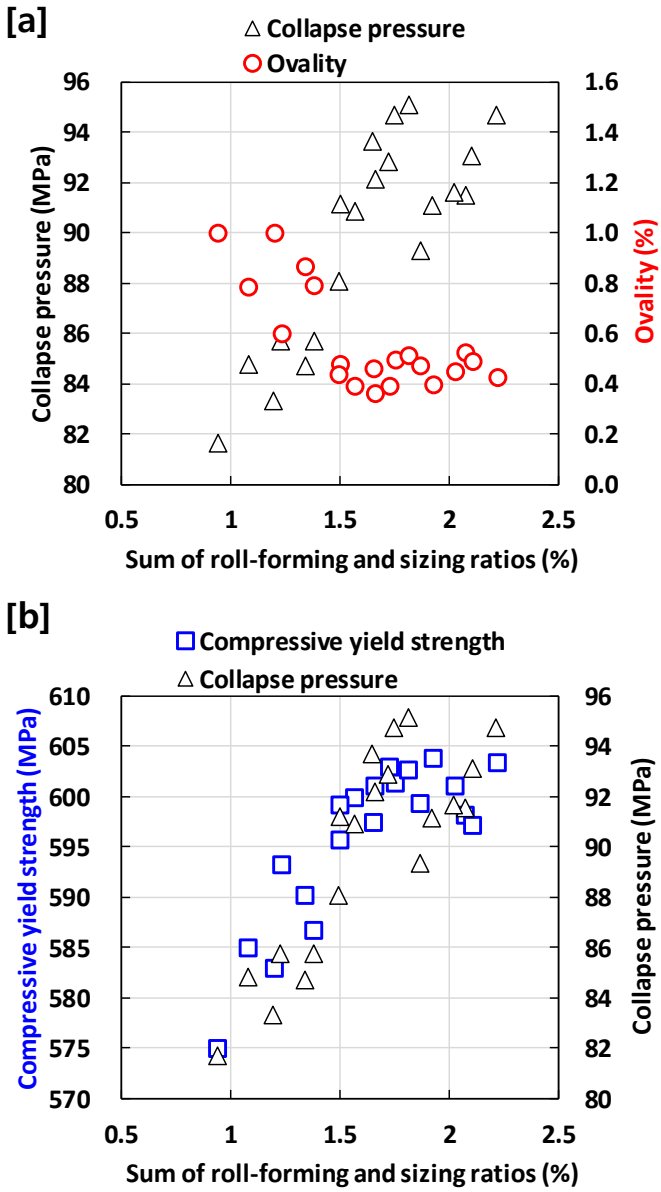

Fig. 4.14. Dependency of sum of roll-forming and sizing ratios on (a) collapse pressure and ovality, and (b) compressive yield strength and collapse pressure

CHAPTER 5

COLLAPSE PERFORMANCE OF ERW PIPE ACCORDING TO DIAMETER TO THICKNESS RATIO

5.1 Key parameter selection

To quantify the effects of key design variables on yield strength and structural performances, parametric study is performed. As mentioned before, diameter, thickness and sizing ratio are highly influential factors among all the relevant design variables. Therefore, these are varied individually as listed in Table 5.1. Values for diameter and thickness are selected embracing current practical usage. The sizing ratio is also varied discretely within a range of values that is considered to be practical for offshore application.

Table 5.1. Cases for parametric study according to diameter and thickness

Case	Width (mm)	Thickness (mm)	Diameter (mm)	*D*/*t*	SZ ratio (%)
1	220	2	75	36	0.2~1.0
2	220	5.460	72	14	
3	780	10	258	26	
4	780	12	260	22	
5	780	14	262	19	
6	980	9.5	312	32	
7	980	11	313	28	
8	1100	14	364	26	
9	1100	23	373	16	
10	1350	19.5	449	23	
11	1600	14.5	524	36	
12	1860	20	612	31	

5.2 Influence factors according to sizing process

If the diameter and thickness are changed, the history of deformation during the manufacturing is different. In other words, even if the compressive strain by the sizing ratio is the same, the circumferential strain by breakdown, flattening and springback varies depending on the D/t. It is necessary to examine how the influence factors on the collapse pressure change after the manufacturing depending on the D/t.

5.2.1 Variation of yield strength according to sizing ratio

In Fig. 5.1, compressive and tensile yield strengths in the circumferential direction of the pipe were evaluated according to the roll-forming and sizing ratios for various D/t. As the sizing ratio increased, the compressive yield strength increased gradually up to 7% compared to that of the steel plate. This is due to strain hardening effect under continuous compression from the finpass process.

On the other hand, the effect of the sizing ratio on the tensile yield strength after the flattening had little effect regardless of D/t. These results can be interpreted that the influences of previously applied plastic forming on tensile yield strength would vanish gradually, as strain hardening effect due to the flattening process becomes governing.

As shown in Figs 5.2-11. the compressive yield strength was increased up to 5% with the increasing sizing ratio regardless of the D/t.

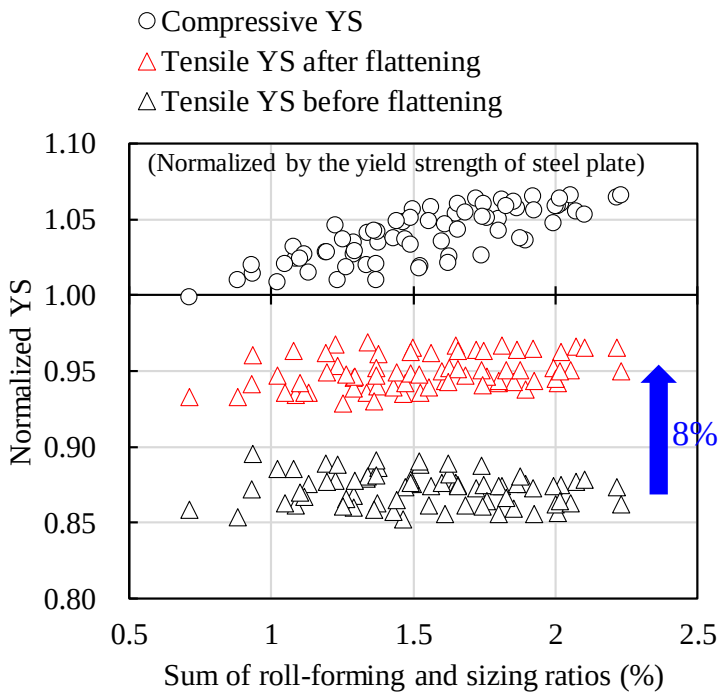

Fig. 5.1. Variations of tensile and compressive yield strengths according to sum of roll-forming and sizing ratios

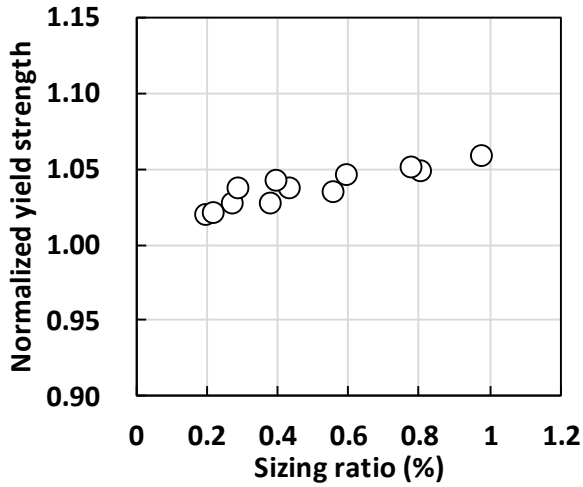

Fig. 5.2. Variations of compressive yield strength according to sizing ratio when *D*/*t*=36 (OD=72 mm, t=2 mm)

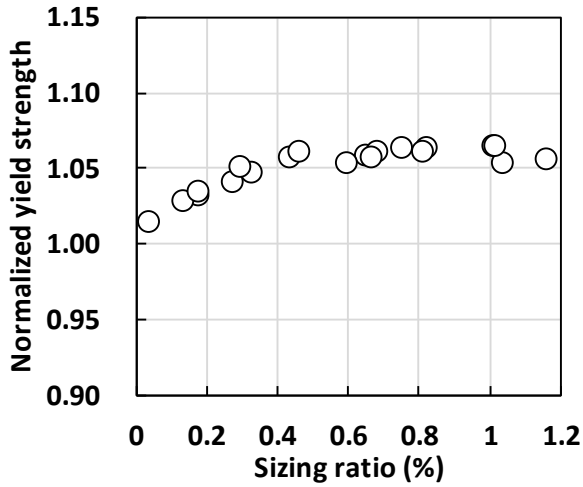

Fig. 5.3. Variations of compressive yield strength according to sizing ratio when *D*/*t*=14 (OD=75 mm, t=5.46 mm)

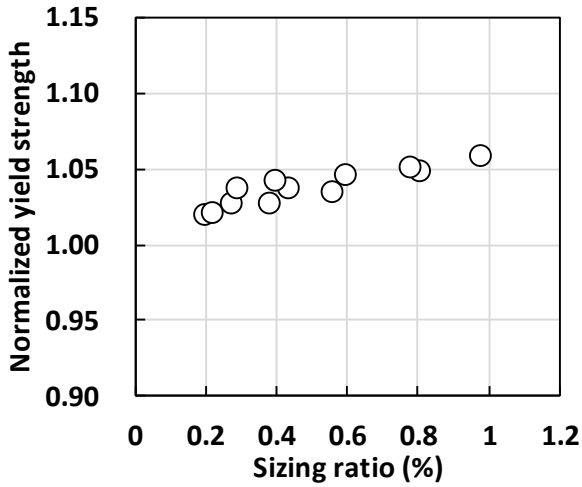

Fig. 5.4. Variations of compressive yield strength according to sizing ratio when *D*/*t*=26 (OD=258 mm, t=10 mm)

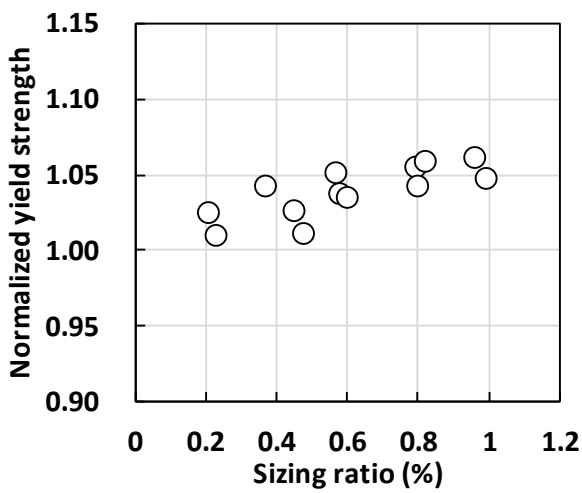

Fig. 5.5. Variations of compressive yield strength according to sizing ratio when *D*/*t*=22 (OD=260 mm, t=12 mm)

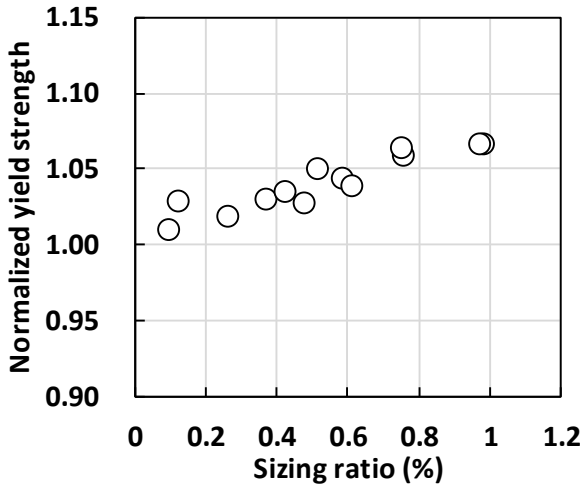

Fig. 5.6. Variations of compressive yield strength according to sizing ratio when *D*/*t*=19 (OD=262 mm, t=14 mm)

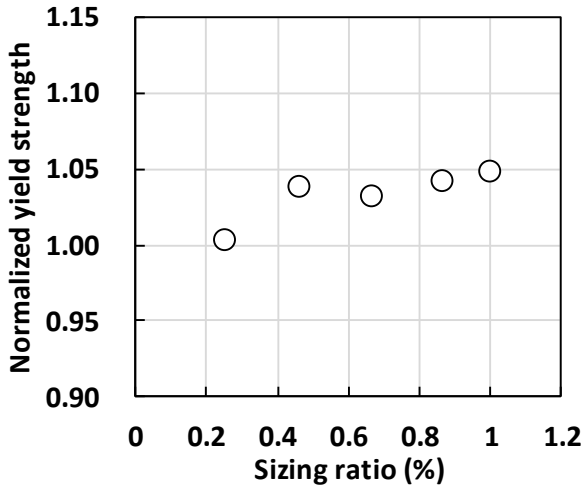

Fig. 5.7. Variations of compressive yield strength according to sizing ratio when *D*/*t*=33 (OD=312 mm, t=9.5 mm)

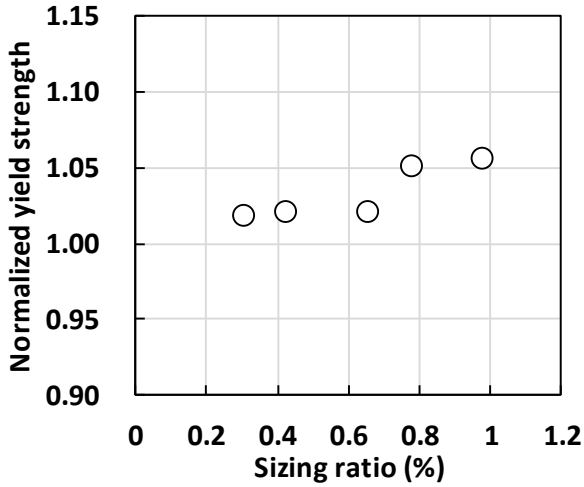

Fig. 5.8. Variations of compressive yield strength according to sizing ratio when *D*/*t*=28 (OD=313 mm, t=11 mm)

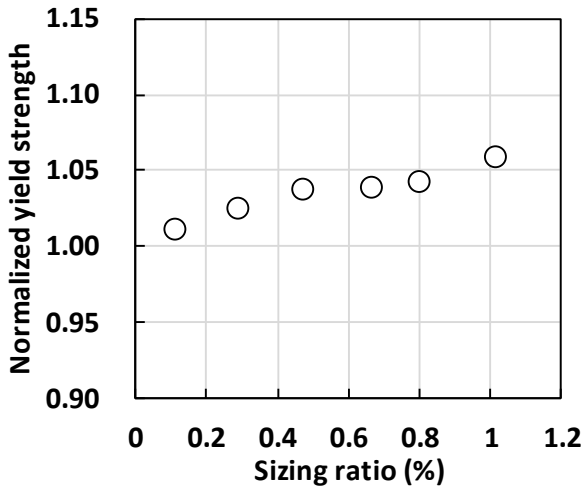

Fig. 5.9. Variations of compressive yield strength according to sizing ratio when *D*/*t*=23 (OD=449 mm, t=19.5 mm)

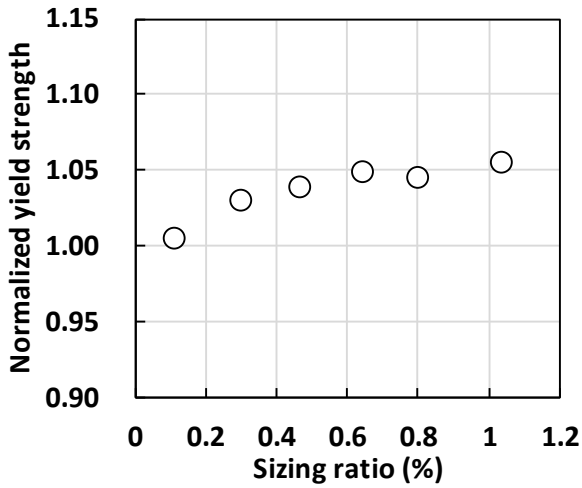

Fig. 5.10. Variations of compressive yield strength according to sizing ratio when *D*/*t*=36 (OD=524 mm, t=14.5 mm)

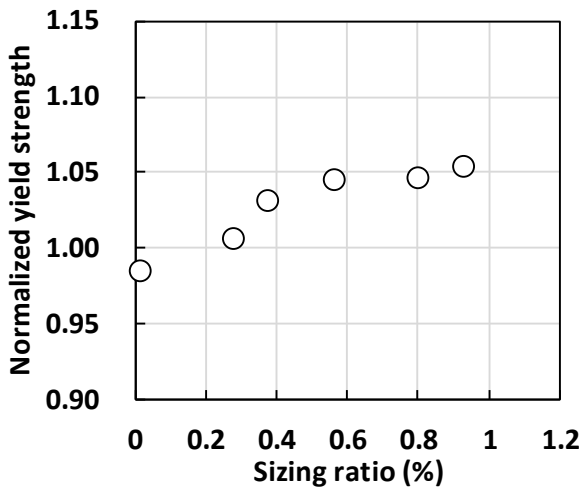

Fig. 5.11. Variations of compressive yield strength according to sizing ratio when *D*/*t*=31 (OD=612 mm, t=20 mm)

5.2.2 Improvement of ovality according to sizing ratios

In Fig. 5.12, the improvement of ovality by the sizing process was evaluated according to the roll-forming and sizing ratios for various D/t. Regardless of D/t, the effect of the sizing process on improvement of ovality according to the sizing ratio was similar. In other words, if the sizing ratio is more than 0.4%, the improved ovality corresponds to 0.3 to 0.6%. Ovality improvement is not related to D/t, and ovality improvement can be affected by roller shape as well as sizing ratio.

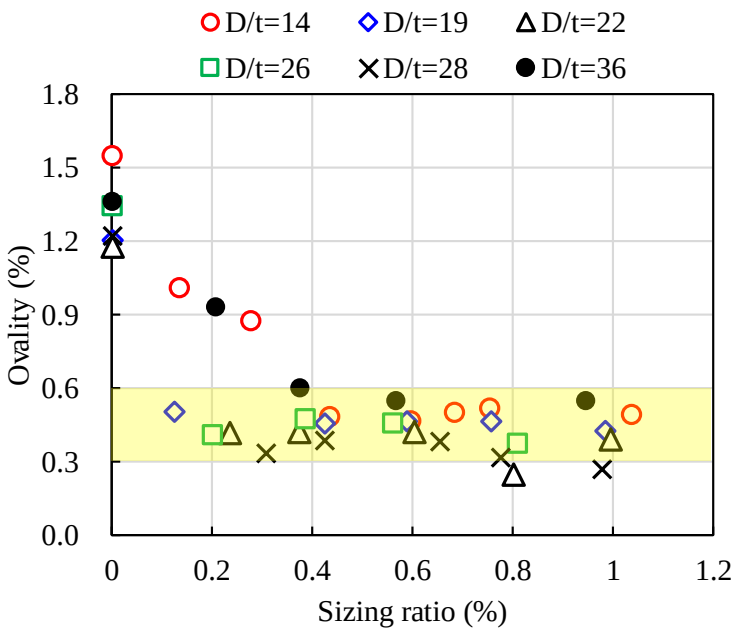

Fig. 5.12. Dependency of sizing ratio on ovality according to *D*/*t*

5.3 Enhancement of collapse performance by sizing process

The collapse pressure decreases with increasing D/t as shown in Fig. 5.13, because the collapse pressure is highly governed by the D/t. Nevertheless, it is evaluated how the tubing process affected the collapse pressure according to D/t.

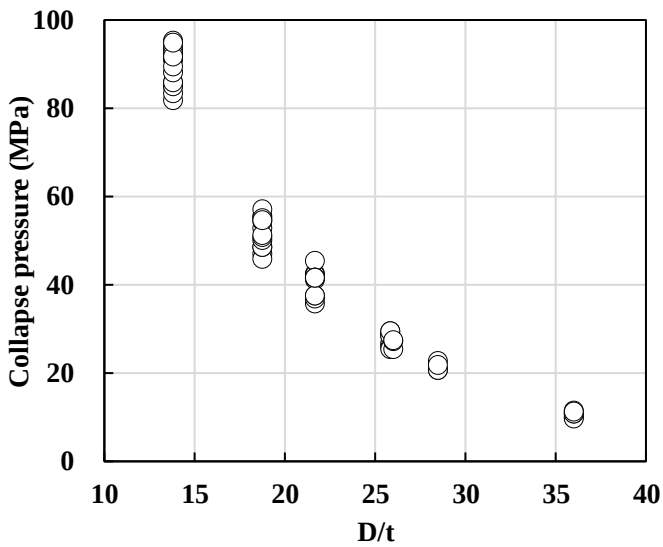

Fig. 5.13. Collapse pressure of ERW pipes according to *D*/*t*

5.3.1 Effect of influence factors according to *D*/*t*

In case of the ovality of 0.3 to 0.6% after the manufacturing, the collapse pressure, which was normalized by the yield pressure defined as Equation (5.1), was compared according to D/t as shown in Fig. 5.14. Regardless of

D/t, there was no clear relationship between the ovality and the collapse pressure. Larger ovality has a greater effect on reducing collapse pressure, but if the ovality is less than 0.6%, not only the ovality but also other influence factors should be considered together.

$$P = 2\sigma_0 \frac{t}{D} \tag{5.1}$$

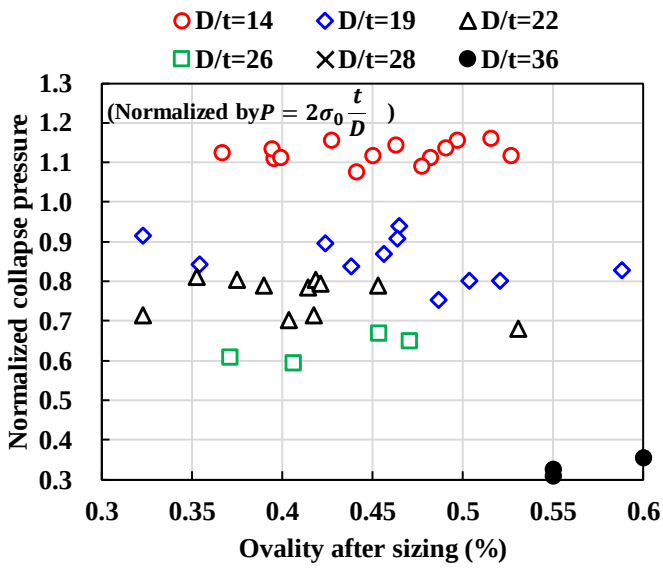

Fig. 5.14. Effect of ovality on collapse pressure according to D/t

On the other hand, the collapse pressure according to the compressive yield strength tends to be different depending on D/t as shown in Figs. 5.15-20. In the case of small D/t, the collapse pressure increased as the compressive yield strength increased as shown in Fig. 5.15. However, in the case of the large D/t, there was no particular relationship between the compressive yield strength and the collapse pressure as shown in Fig. 5.20. This is because the

thinner pipe with increasing D/t buckles elastically, which is more dominant in the geometry such as ovality than the compressive yield strength.

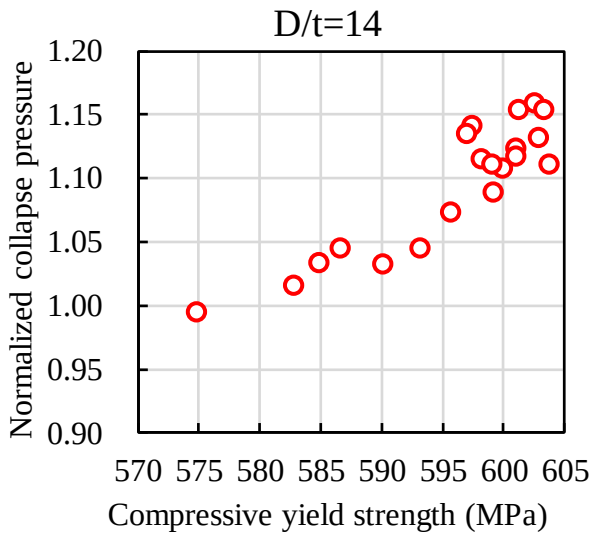

Fig. 5.15. Effect of compressive yield strength on collapse pressure when *D*/*t*=14

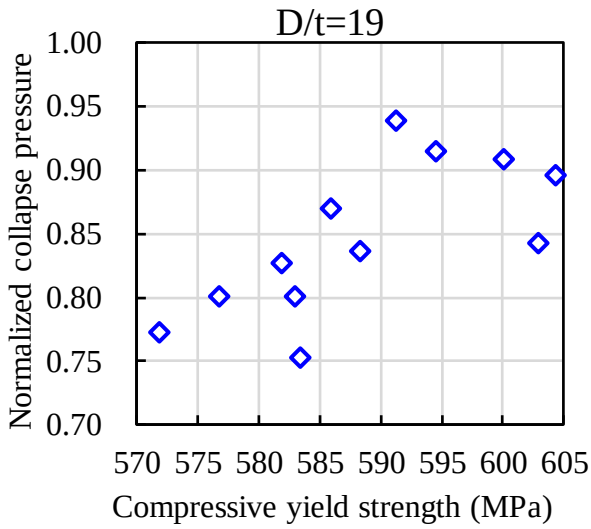

Fig. 5.16. Effect of compressive yield strength on collapse pressure when *D*/*t*=19

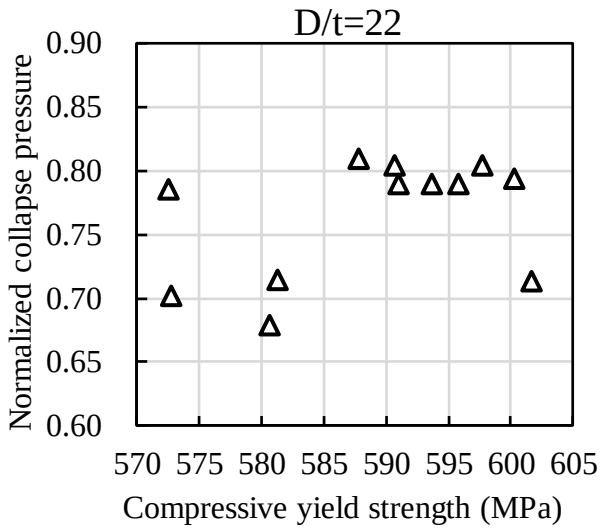

Fig. 5.17. Effect of compressive yield strength on collapse pressure when *D*/*t*=22

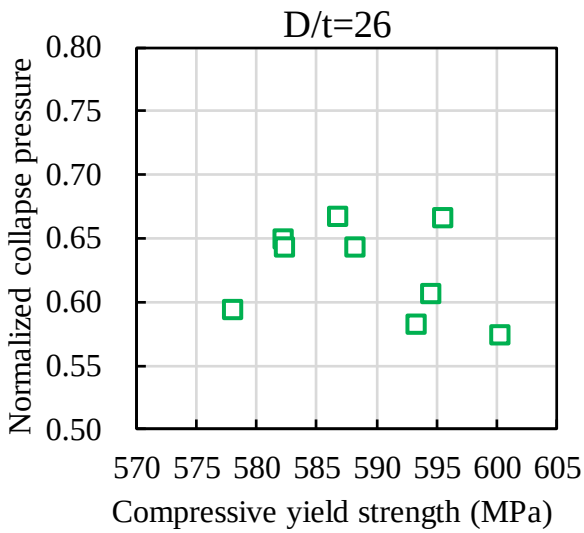

Fig. 5.18. Effect of compressive yield strength on collapse pressure when *D*/*t*=26

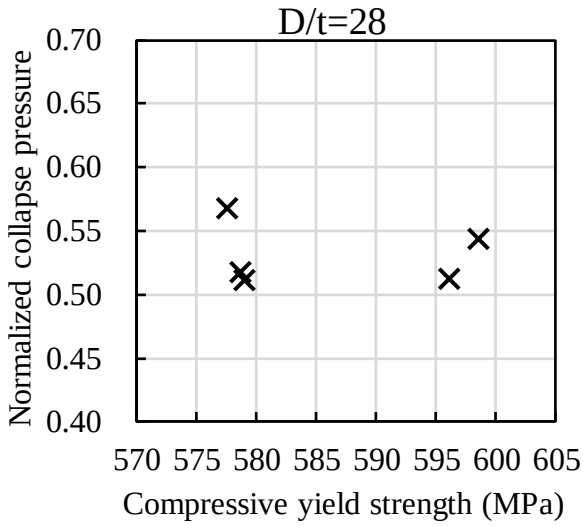

Fig. 5.19. Effect of compressive yield strength on collapse pressure when *D*/*t*=28

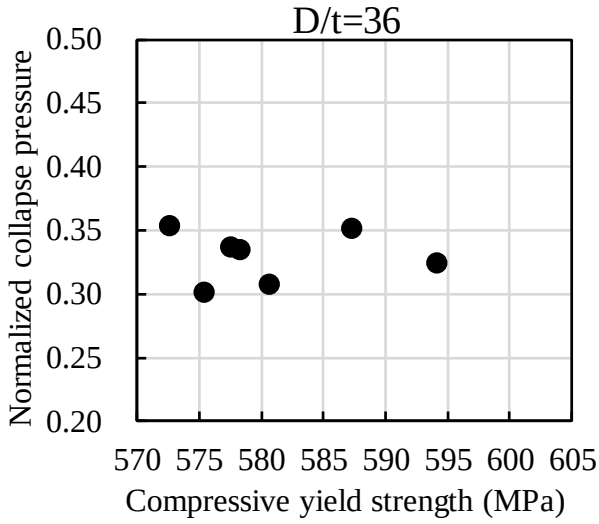

Fig. 5.20. Effect of compressive yield strength on collapse pressure when *D*/*t*=36

5.3.2 Effect of sizing process according to *D*/*t*

Like the effect of the compressive yield strength, the collapse pressure according to the sizing ratio tends to be different depending on D/t as shown in Figs. 5.21-26. At small D/t, the collapse pressure increased with increasing sizing ratio. In particular, when the D/t is 14, the collapse pressure showed a difference of up to 15% depending on the sizing ratio. On the other hand, in the case of large D/t, the effect of the sizing ratio on collapse pressure was insignificant. Increase of D/t brings further reduction in collapse pressure as buckling mode of the pipe turns to elastic buckling from this point, due to relatively slender geometry of the pipe. larger. But, the effect of ovality improvement by the sizing process is similar when the sizing ratio is 0.4% or more. On the contrary the effect of the sizing process on collapse pressure is more considerable for lower D/t pipes since they buckle in the plastic range.

In the case of lower D/t, increasing the sizing ratio helps to improve the collapse performance. In the case of large D/t, the sizing ratio of more than 0.4% has no meaning in improvement of the collapse performance.

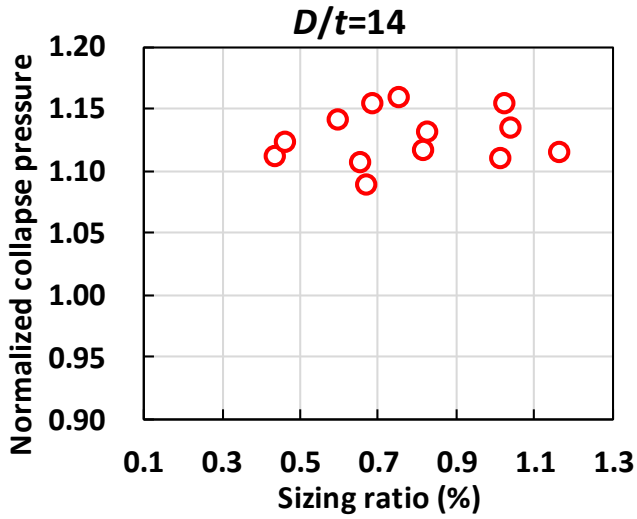

Fig. 5.21. Effect of sizing ratio on collapse pressure when *D*/*t*=14

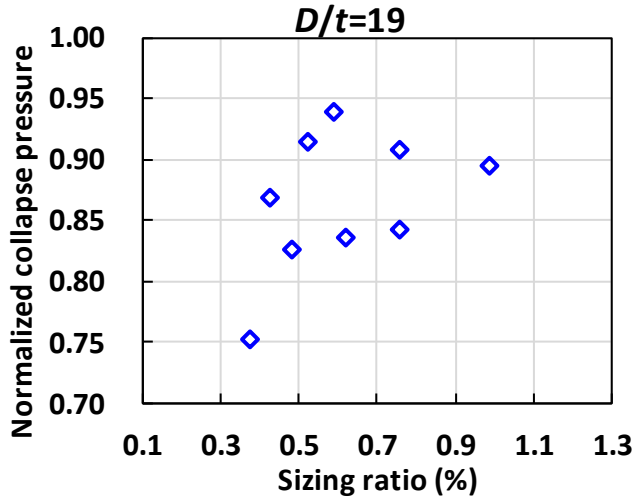

Fig. 5.22. Effect of sizing ratio on collapse pressure when *D*/*t*=19

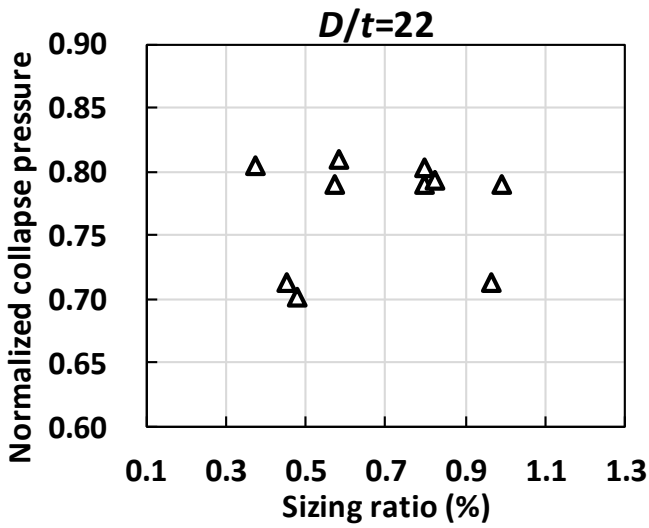

Fig. 5.23. Effect of sizing ratio on collapse pressure when *D*/*t*=22

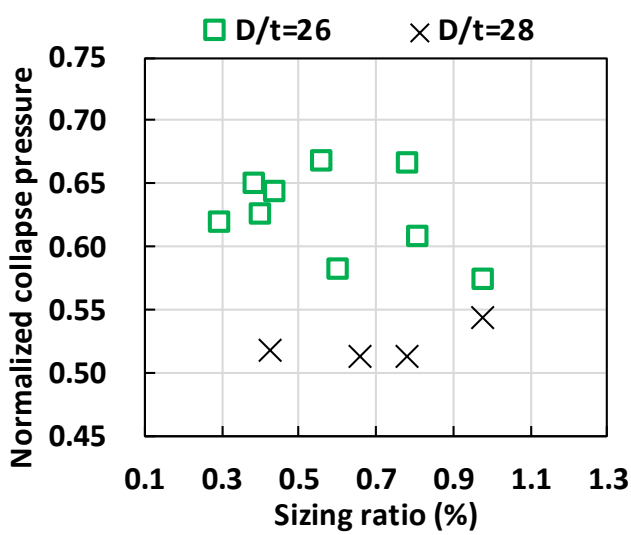

Fig. 5.24. Effect of sizing ratio on collapse pressure when *D*/*t*=26 and 28

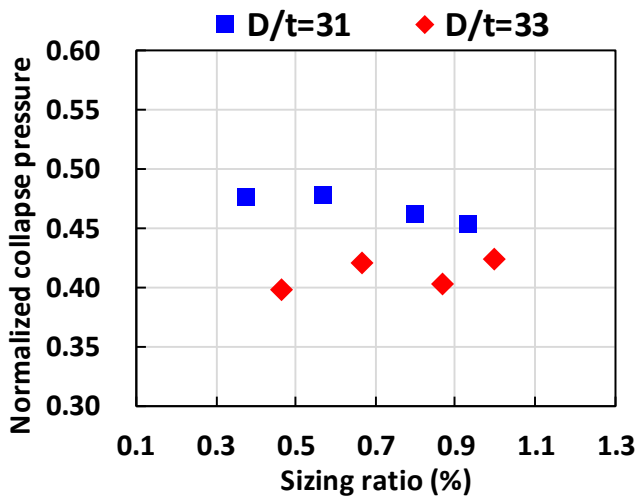

Fig. 5.25. Effect of sizing ratio on collapse pressure when *D*/*t*=31 and 33

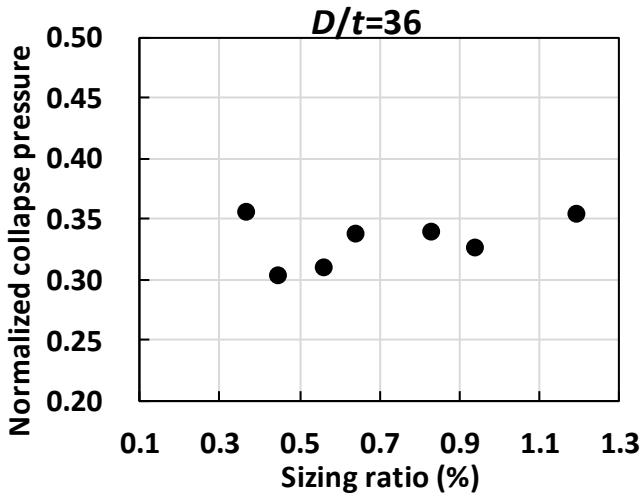

Fig. 5.26. Effect of sizing ratio on collapse pressure when *D*/*t*=36

5.4 Comparison between analysis results and design criteria

In the previous chapter, it was found that the smaller the D/t, the greater the advantage of the sizing process on the collapse pressure. This chapter examines the advantages of the sizing process in detail by comparing the analysis results with design criteria.

5.4.1 Design criteria for collapse pressure

The design criteria proposed the collapse pressures for offshore pipelines in DNV-OS-F101 and API RP 1111, and for tubing and casing in API 5C3 and ISO 10400. API 5C3 developed an empirical formula based on the results of about 2500 experiments and proposed a total of four collapse pressure equations according to the buckling mode (i.e., yield strength, plastic, transition and elastic collapses) as defined in Equations (5.2) to (5.5).

$$P_{c1} = 2 \cdot f_y \left[\frac{(D/t) - 1}{(D/t)^2}\right] \tag{5.2}$$

$$P_{c2} = f_y \cdot \left[\frac{A}{(D/t)} - B\right] - C \tag{5.3}$$

$$P_{c3} = f_y \cdot \left[\frac{F}{(D/t)} - G\right] \tag{5.4}$$

$$P_{c4} = \frac{46.95 \cdot 10^6}{(D/t) \cdot [(D/t) - 1]^2} \tag{5.5}$$

In Equations (5.5) to (5.5), P_{c1}, P_{c2}, P_{c3} and P_{c4} are yield strength collapse, plastic collapse, transition collapse and elastic collapse, respectively. The coefficients are calculated by the Equations (5.6) to (5.10)

$$A = 2.8762 + 0.10679 \times 10^{-5} \times f_y + 0.21301 \times 10^{-10} \times {f_y}^2 - 0.53132 \times 10^{-16} \times {f_y}^3 \quad (5.6)$$

$$B = 0.026233 + 0.50609 \times 10^{-6} \times f_y \quad (5.7)$$

$$C = -465.93 + 0.030867 \times f_y - 0.10483 \times 10^{-7} \times {f_y}^2 - 0.53132 \times 10^{-16} \times {f_y}^3 \quad (5.8)$$

$$F = 2.8762 + 0.10679 \times 10^{-5} \times f_y + 0.21301 \times 10^{-10} \times {f_y}^2 - 0.53132 \times 10^{-16} \times {f_y}^3 \quad (5.9)$$

$$G = FB/A \quad (5.10)$$

The boundaries between each collapse pressure formula are defined by Equations (5.11) to (5.13)

$$(D/t)_{yp} = \frac{\sqrt{(A-2)^2 + 8\left(B + C/f_y\right)} + (A-2)}{2\left(B + C/f_y\right)} \quad (5.11)$$

$$(D/t)_{PT} = \frac{f_y(A-F)}{C + f_y(B-G)} \quad (5.12)$$

$$(D/t)_{TE} = \frac{2 + B/A}{3\,B/A} \quad (5.13)$$

ISO 10400, on the other hand, proposes one formula regardless of the buckling modes, and includes two factors to consider the effects of the pipe manufacturing process as defined in Equation (5.14).

$$P_{des} = \frac{\left(P_{edes} + P_{ydes}\right) - \left[\left(P_{edes} - P_{ydes}\right)^2 + 4P_{edes} \cdot P_{ydes} \cdot H_{tdes}\right]^{1/2}}{2(1 - H_{tdes})} \quad (5.14)$$

In Equation (5.14), H_{tdes} is residual stress influence factor. P_{ydes} and P_{edes} are collapse yield strength and ultimate collapsing strength of geometric elastic destabilization, respectively, and defined as Equations (5.15) and (5.16).

$$P_{ydes} = K_{ydes} \cdot 2f_y(t/D)[1 + t/(2D)] \quad (5.15)$$

$$P_{edes} = 0.825 \cdot 2E/\{(1 - \nu^2)(t/D)[D/t - 1]^2\} \quad (5.16)$$

In Equation (5.15), K_{ydes} is yield strength reduction factor.

The first factor, H_{tdes}, takes into account the effects of residual stress, and the another one, K_{ydes}, considers reduction of yield strength due to manufacturing process which reduce the yield strength by up to 17%.

API RP 1111 also proposes one formula as defined in Equations (5.17) and (5.18), and includes the collapse factor to consider the effects of the

manufacturing process which means the initial geometric imperfections, residual stress and change in the yield strength.

$$f_o P_c \geq (P_o - P_i) \tag{5.17}$$

$$P_c = \frac{P_y P_e}{\sqrt{{P_y}^2 + {P_e}^2}} \tag{5.18}$$

In Equation (5.17), P_o, P_i, P_c and f_o are external pressure, internal pressure, collapse pressure and collapse factor, respectively. In Equation (5.18), P_y and P_e are yield pressure at collapse and elastic collapse pressure, respectively and defined as Equations (5.19) and (5.20).

$$P_y = 2f_y(t/D) \tag{5.19}$$

$$P_e = 2E\frac{(t/D)^3}{(1-\nu^2)} \tag{5.20}$$

In the case of the ERW and UOE pipes, the collapse pressures are reduced by 30% and 40%, respectively by the collapse factor.

As defined in Equations (5.21) and (5.22), DNV-OS-F101 proposes a fabrication factor to consider the difference in tensile and compressive yield strength after the pipe manufacturing process.

$$\frac{P_c}{\gamma_m \gamma_{SC}} \geq (P_o - P_i) \tag{5.21}$$

$$(P_c - P_{el}) \cdot \left({P_c}^2 - {P_p}^2\right) = P_c \cdot P_{el} \cdot P_p \cdot f_0 \cdot (D/t) \tag{5.22}$$

In Equation (5.21), γ_m and γ_{SC} are material resistance factor and safety class resistance factor, respectively. In Equation (5.22), P_{el} and P_p are elastic collapse pressure and plastic collapse pressure, respectively and defined as Equations (5.23) and (5.24).

$$P_{el} = 2E(t/D)^3/(1 - \nu^2) \tag{5.23}$$

$$P_p = f_y \cdot \alpha_{fab} \cdot (2t/D) \tag{5.24}$$

In Equation (5.24), α_{fab} is the fabrication factor. For ERW pipes, the maximum fabrication factor is 0.93 which means 17% reduction of plastic collapse pressure.

The current collapse strength design formulas do not consider enhancement of the collapse pressure by the sizing of the ERW pipe manufacturing process. In the case of the ERW pipes with small D/t (i.e., thicker pipes affected by the yield strength), the collapse pressure is suggested conservatively because the increase in circumferential compressive yield strength due to the sizing process is not considered.

5.4.2 Advantage of sizing process according to D/t

As shown in Fig. 5.27, the analysis results and the design criteria were compared to evaluate the benefits of the sizing process on the collapse pressure. The analysis results have collapse pressure distributions by applying different sizing ratios for the same D/t. The analysis results generally follow the design criteria for offshore pipeline rather than for casing and tubing. In the case of large D/t which has little influence of the stress-strain relationship, the analysis results were well matched with API RP 1111 and DNV-OS-F101 indicating that the analysis result is reliable. On the other hand, for the smaller D/t more influenced by the stress-strain curve, the difference between the design criteria and the analysis results, which do not reflect the benefits of the sizing process, has increased significantly.

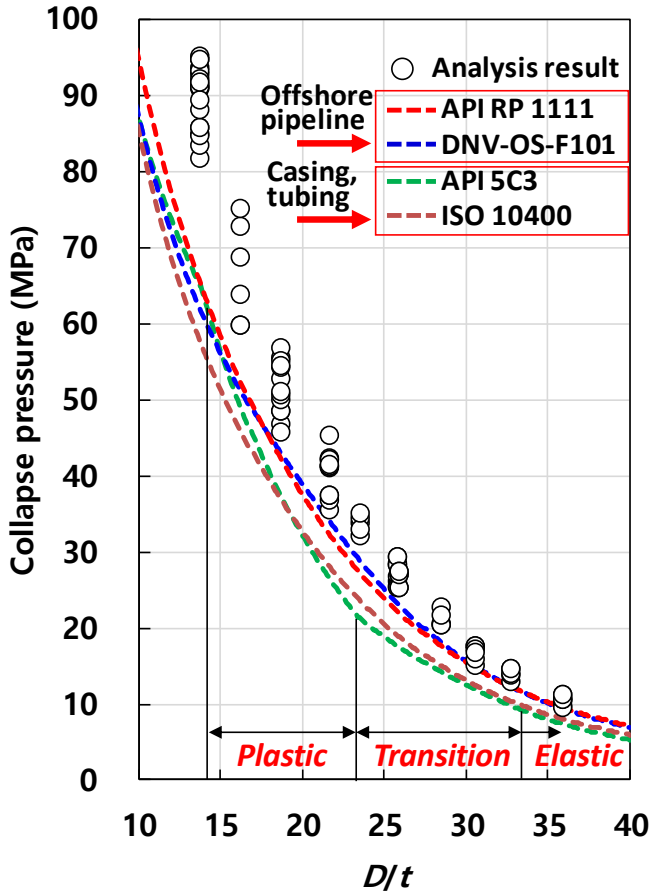

Fig. 5.27. Comparison analysis results with design criteria

5.4.3 Suggestion of sizing ratio for collapse pressure

Based on the results of this study, it was tried to suggest an appropriate sizing ratio for improving collapse pressure. As shown in Fig. 5.28, ovality, compressive yield strength, and collapse strength were compared together for a thick ERW pipe (D/t=14) which is greatly affected by the sizing process. The improvement of ovality was insignificant above 0.4% of the sizing ratio, while the compressive yield strength increased continuously with increasing sizing ratio. However, the increase rate of the compressive yield strength was

significantly decreased above 0.4% of the sizing ratio. The distribution of ovality and the compressive yield strength according to the sizing ratio directly affected the collapse pressure. When 0.4% of the sizing ratio was applied, the collapse pressure was increased by 10%, whereas when 0.4% or more of the sizing ratio was applied, the increase in the collapse pressure was insignificant. In other words, 0.4% can be suggested as the minimum sizing ratio to improve the collapse pressure.

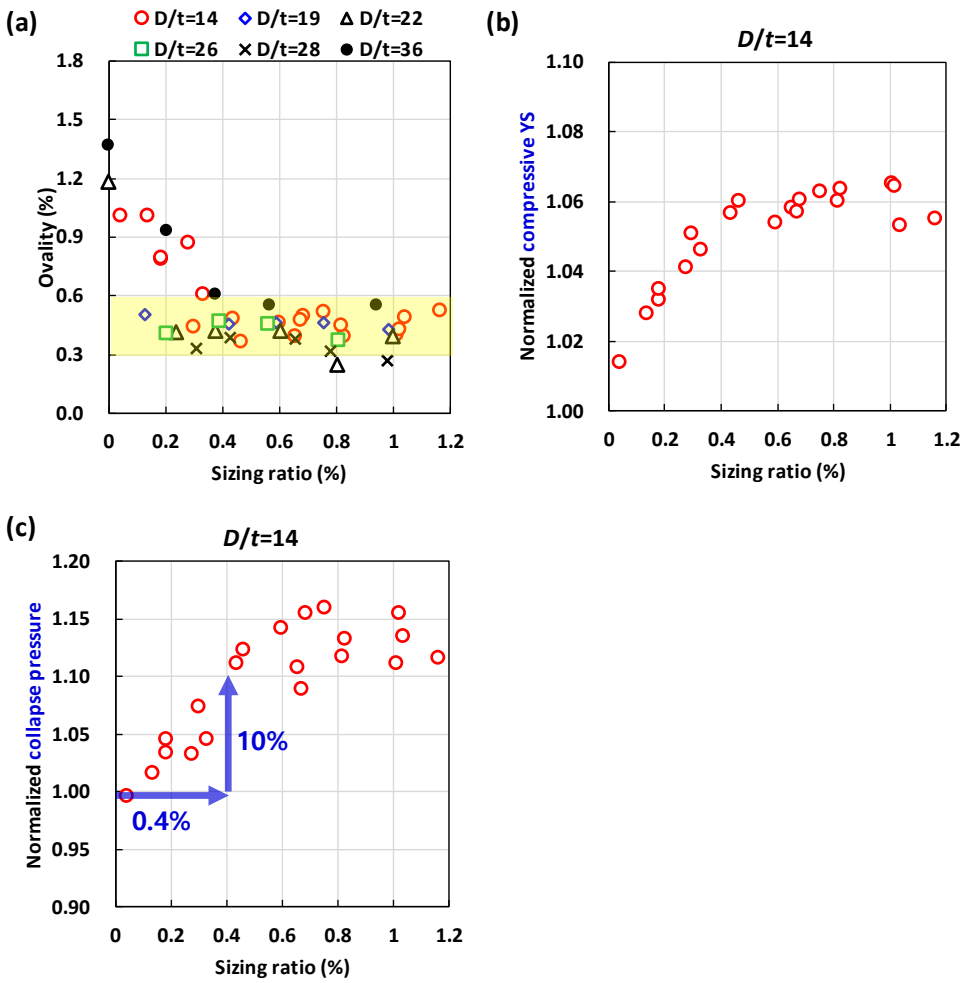

Fig. 5.28. (a) Ovality, (b) compressive yield strength and (c) collapse pressure according to sizing ratio

The analysis result applying the sizing ratio of 0.4% or more are shown in Fig. 5.29. The advantage of the sizing process on collapse pressure are also clearly shown, and for the pipe of D/t=14 the collapse pressure has a margin of 37% against to design criteria.

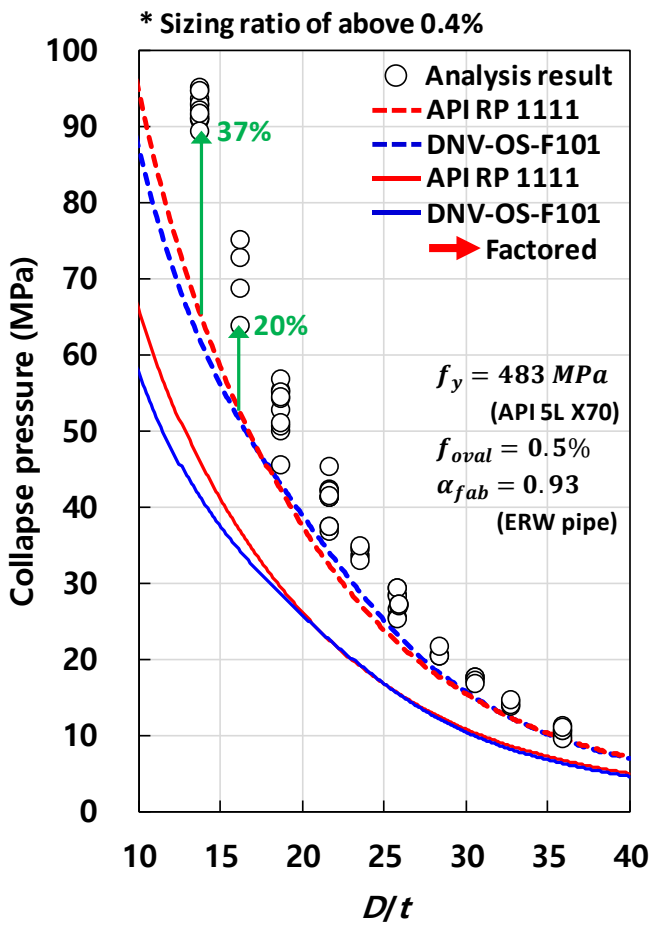

Fig. 5.29. Enhancement of collapse pressure by applying sizing ratio of 0.4% or more

Enhancement of the collapse pressure by the sizing process was also analyzed as shown in Fig. 5.30. The compressive stress-strain relationship was modified by the stress-strain hardening during the sizing process, and difference of stress-strain relationships between before and after the ERW pipe manufacturing process gradually increased after yielding. The local buckling under external pressure occurred above the yielding leading to increase of the collapse pressure.

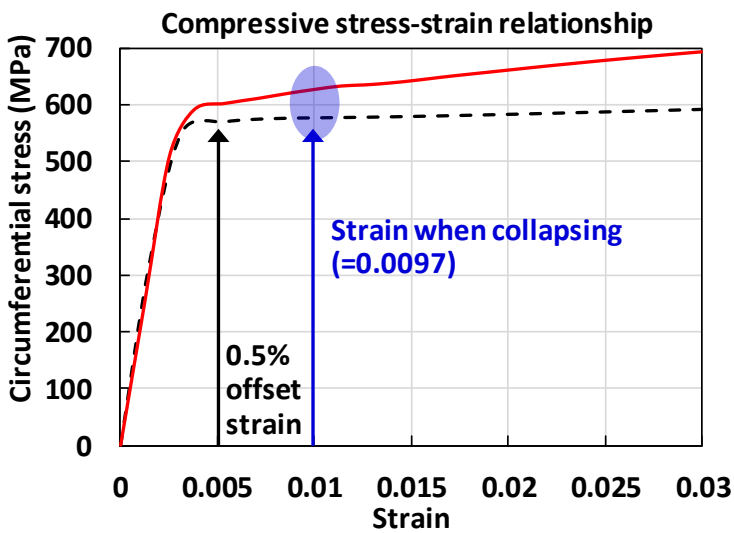

Fig. 5.30. Enhancement of collapse pressure by modified stress-strain relationship

CHAPTER 6

CONCLUSIONS AND RECOMMENDATIONS FOR FURTHER STUDY

An analytical approach based on the geometric information using the three-dimensional FEM is proposed to simulate the roll-forming and sizing processes in manufacturing process of the ERW pipe. Whole processes, including the breakdown, finpass, squeezing and sizing processes, were simulated by continuous analysis incorporating the material model with the Bauschinger effect and strain hardening. Using the developed analytical approach, change in yield strength, geometric imperfection and residual stress throughout the roll-forming and sizing ratios were tracked.

For the computational simulation, a combined hardening model describing the repeated loading and unloading during the ERW pipe manufacturing process was adopted. The adopted material model, which is the Modified Chaboche model, was fitted using the cyclic loading test result of API 5L X70. It was shown that strain hardening, Bauschinger effect, yield plateau and evolution of Young's modulus developed during the manufacturing process can be considered in the simulation adequately.

A platform for predicting collapse pressure considering the ERW pipe manufacturing process is developed. This platform is a three-dimensional FEA immediately following the simulation result of the ERW pipe manufacturing process. The parametric study is conducted to examine the

influence of the design variables on the collapse performance. The following findings could be drawn from the study

Among the manufacturing process of the ERW pipe, the sizing has significant effects on improvement of the geometric imperfection such as out-of-roundness and increase of the compressive yield strength in circumferential direction by as much as 5%. In particular, the effects of the sizing process on the ovality and the compressive yield strength depends on the sizing ratio. The compressive yield strength continued to increase with the increasing sizing ratio, while the improvement of ovality was insignificant above the sizing ratio of 0.4%. The characteristics of the influence variable according to the sizing process directly affected the collapse pressure. For larger D/t, effect of the sizing process on the collapse performance is minor because the pipe shows elastic buckling mainly influenced by the geometric imperfection. On the contrary, enhancement of the collapse performance by the sizing process is more effective for smaller D/t due to the increased compressive yield strength. However, the sizing process exerts a reducing effect on the tensile yield strength due to Bauschinger effect for all the examined cases. Therefore, the sizing process has to be treated carefully when it comes to quality control of the pipe.

The collapse analysis result is compared with design criteria to check the advantage of the sizing process. The analytical result showed a significant difference from the design criteria for thick pipes (i.e., small D/t). This

difference is due to the fact that the current design criteria do not consider the benefits of the sizing process on collapse pressure.

The numerical model for simulating the roll-forming and sizing process of ERW pipe provides insight into the relationship between collapse performance and manufacturing parameters such as the sizing ratio. However, the result of this study was derived only based on the analysis. Further study should focus on comparison and calibration of the numerical results via experimental validation. Also, based on the analysis results, it is necessary to propose design guideline for increase of the collapse pressure satisfying the quality of the pipe with regard to the sizing ratio or diameter and thickness.

REFERENCE

Al-Showaiter, A., Taheri, F., & Kenny, S. (2008). Influence of pipeline misalignment on the local buckling response. Paper presented at the 2008 7th International Pipeline Conference.

ASTM E9 (2012). Standard test methods of compression testing of metallic materials at room temperature. 98-105.

ASTM A370 (2012). Standard test methods and definitions for mechanical testing of steel products.

Bastola, A., Wang, J., Mirzaee-Sisan, A., & Njuguna, J. (2014). Predicting hydrostatic collapse of pipes using finite element analysis. Paper presented at the ASME 2014 33rd International Conference on Ocean, Offshore and Arctic Engineering, San Francisco, California, USA.

Berglund, J., Brown, C. A., Rosen, B.-G., & Bay, N. (2010). Milled die steel surface roughness correlation with steel sheet friction. CIRP Annals - Manufacturing Technology, 59(1), 577-580.

Chaboche, J. L., & Rousselier, G. (1983). On the plastic and viscoplastic constitutive equations—Part I: Rules developed with internal variable concept. *Journal of Pressure Vessel Technology*, 105(2), 153-158.

Chen, W. F., & Ross, D. A. (1978). Tests of fabricated tubular columns. September 1978, Fritz Laboratory Reports, Paper 478.

Fraldi, M., & Guarracino, F. (2013). Towards an accurate assessment of UOE pipes under external pressure: Effects of geometric imperfection and material inhomogeneity. *Thin-Walled Structures*, 63, 147-162.

Han, S.-W., Park, Y. C., Kang, S.-C., Jung, S., Kim, H.-K. (2019). Collapse Analysis of ERW Pipe Based on Roll-Forming and Sizing Simulations. *Journal of Marine Science and Engineering*, 7(11), 410.

Herynk, M., Kyriakides, S., Onoufriou, A., & Yun, H.D. (2007). Effects of the UOE/UOC pipe manufacturing processes on pipe collapse pressure. *International Journal of Mechanical Sciences*, 49(5), 533-553.

Institute, A. P. (2012). API 5L: Specification for Line Pipe. In. Washington, DC, USA.

Jung-Ho, C., & Noboru, K. (1985). An analysis of metal forming processes using large deformation elastic-plastic formulations. *Computer Methods in Applied Mechanics and Engineering*, 49(1), 71-108.

Kyriakides, S., & Corona, E. (2007). Mechanics of offshore pipelines: volume 1 buckling and collapse (Vol. 1): Elsevier.

Kyriakides, S., Corona, E., & Fischer, F. (1994). On the effect of the UOE manufacturing process on the collapse pressure of long tubes.

Lee, J., Kim, D., Quagliato, L., Kang, S., & Kim, N. (2017). Change of the yield stress in roll formed ERW pipes considering the Bauschinger effect. *Journal of Materials Processing Technology*, 244, 304-313.

McConnell, C., & Lenard, J. G. (2000). Friction in cold rolling of a low carbon steel with lubricants. *Journal of Materials Processing Technology*, 99(1-3), 86-93.

Moen, C. D., Igusa, T., & Schafer, B. W. (2008). Prediction of residual stresses and strains in cold-formed steel members. *Thin-Walled Structures*, 46(11), 1274-1289.

Murphey, C., & Langner, C. (1985). Ultimate pipe strength under bending, collapse and fatigue. Paper presented at the Proceedings of the 4th International Conference on Offshore Mechanics and Arctic Engineering.

Nagata, Y., & Tsuru, E. (2016). Geometry and Collapse Pressure of HF-ERW Line Pipe Reel-laid in Deepwater. Paper presented at the The 26th International Ocean and Polar Engineering Conference, Rhodes, Greece.

Nishimura, N., Takeuchi, S., Murakami, S., & Sanui, K. (1997). The Effect Manufacturing Processes on Residual Stress and Yield Stress of ERW Pipes. Kou kouzou rombunshuu, 4(13), 53-62.

Ostapenko, A., & Gunzelman, S. X. (1975). Local buckling tests on two high-strength steel tubular columns, July 1975. Fritz Laboratory Reports. Paper 2172.

Ostapenko, A., & Gunzelman, S. X. (1978). Local Buckling Tests on Three Steel Large-diameter Tubular Columns. International Specialty Conference on Cold-Formed Steel Structures. 7.

Ostapenko, A., & Grimm, D.F. (1980). Local buckling of cylindrical tubular columns made of a-36 steel. February 1980. Fritz Laboratory Reports. Paper 2234.

Ross, D. (1978). The strength and behavior of fabricated tubular steel columns. Ph.D. Thesis, Lehigh University.

Roy, S. (2006). Experimental and analytical evaluation of enhancement in fatigue resistance of welded details subjected to post-weld ultrasonic impact treatment. (Ph.D. Thesis), Lehigh University,

Tsuru, E., Tomioka, K., Shitamoto, H., Ozaki, M., Karjadi, E., Boyd, H., & Demmink, H. (2015). Collapse Resistance of HF-ERW Line Pipe Installed

in Deepwater by R-Lay. Paper presented at the The 25th International Ocean and Polar Engineering Conference, Kona, Hawaii, USA.

Xie, P., Zhao, Y., Yue, Q., & Palmer, A. C. (2015). Dynamic loading history and collapse analysis of the pipe during deepwater S-lay operation. *Marine Structures*, 40, 183-192.

Yeh, M., & Kyriakides, S. (1986). On the collapse of inelastic thick-walled tubes under external pressure.

Yi, J. (2017). Optimal Design Procedure for Offshore Pipelines based on Computational Simulation of Pipe Forming Process. Ph.D. Thesis, Seoul National University.

Yoshida, F., Uemori, T., & Fujiwara, K. (2002). Elastic–plastic behavior of steel sheets under in-plane cyclic tension–compression at large strain. *International Journal of Plasticity*, 18(5-6), 633-659.

Zou, T., Li, D., Wu, G., Peng, Y., & Design. (2016). Yield strength development from high strength steel plate to UOE pipe. *Material and Design, 89*, 1107-1122.

국 문 초 록

한성욱
건설환경공학부
서울대학교 대학원

최근 에너지 산업이 발달하고 심해의 천연자원 생산이 증가함에 따라, 고성능 파이프라인의 수요가 점점 증가하고 있다. 해저 파이프라인은 극한의 수압에 저항할 수 있어야 하는데, 여러 종류의 강관 중에서 Electric Resistance Welded (ERW) 강관은 용접부의 취약성으로 인해 해저 파이프라인 보다는 지상의 파이프라인 또는 유정관으로 주로 활용되어 왔다. 용접기술의 발달과 함께 ERW 강관도 해저 파이프라인으로 활용 가능하다는 연구가 점점 진행되고 있으나, 산업계에서는 ERW 강관에 대한 연구가 미비하여 해저파이프라인으로 사용하는데 아직까지 주저하고 있다.

ERW 강관의 장점과 단점은 조관공정으로부터 확인할 수 있다. ERW 강관 조관공정의 특징은 조관 전부터 조관이 완료되는 시점까지 연속적인 공정으로 이루어지는 것이다. 이러한 특징으로 인해 ERW 강관은 다른 종류의 강관에 비해 생산성이 뛰어난 반면, 제조공정 중 발생하는 현상을 각 공정마다 정확히 추적하기 힘들기 때문에 다음과 같은 문제를 야기한다.

첫 번째는, 조관 중 발생하는 소성변형으로 인해 변화된 항복강도를 예측하기 힘들다. 조관 중 발생하는 반복적인 재하-제하-재부하가 변형경화와 바우싱거 효과를 일으키며, 이는 응력-변형률 선도를 변화시켜 조관 후 항복강도를 증가 또는 감소시킨다. 항복강도의 변화는 강관의 구조성능에 직접적인 영향을 미칠 뿐만 아니라, 조관 후 항복강도는 강관의 품질 평가에 활용되는 대표적인 지표이기 때문에 정확한 추적이 필요하다. 두 번째는, 조관 중 발생한 기하학적 결함과 잔류응력이다. 조관 후 단면의 진원도와 잔류응력 또한 강관의 구조성능에 직접적인 영향을 미치며, 조관공정에 따라 이를 정확히 예측하는 것이 과다설계를 예방하는 방법 중 하나이다. 조관공정 추적의 한계로 인해 각각의 조관사는 조관공정에 대한 노하우를 가지고 있다. 이로 인해 조관공정에 대한 정보는 매우 제한적이며, 동일한 강관을 조관하여도 서로 다른 조관 노하우를 적용하기 때문에 조관 후 변화된 항복강도가 다르며, 구조성능에 대한 차이를 보인다.

본 논문에서는 3차원 유한요소해석을 통해 ERW 강관의 조관공정을 시뮬레이션 하였다. 수치해석의 정확도를 향상시키기 위해 복합 소성 재료 모델을 유한요소모델에 적용하였다. 적용된 재료모델은 가공경화, 바우싱거 효과뿐만 아니라 항복고원 및 탄성계수의 변화도 모사하였다.

ERW 강관의 조관공정 중에서 Roll-forming 과 Sizing 공정이 시뮬레이션 되었으며, 원주방향으로 압축력이 가해지는 Finpass 와 Sizing 공정이 조관변수로 고려되었다. 조관변수에 따라 항복강도, 진원도 및 잔류응력의 변화를 검토하였으며, 조관공정의 영향을

반영하기 위해 조관 해석이 완료된 강관 해석모델을 그대로 활용하여 붕괴성능을 평가하였다. 또한, 매개변수 해석을 통해 강관의 직경과 두께에 따라 항복강도, 진원도 및 붕괴 성능에 미치는 조관변수의 영향을 규명하였다.

ERW 강관 조관공정 중 Sizing 공정의 영향이 지대하였는데, Sizing을 통해 단면의 진원도가 향상되었으며, 압축항복강도는 증가하고 인장항복강도는 감소하였다. 특히, 원주방향으로 가해지는 압축력이 증가할수록 변형경화에 의해 압축항복강도가 점점 증가하였고, 인장항복강도는 점점 감소하였으나, Flattening 후 인장항복강도에는 Sizing 공정의 영향이 미미하였다. 반면, 0.4% 이상의 Sizing ratio에서는 Sizing에 의한 진원도 개선 효과의 차이가 미미하였다.

Sizing에 의해 진원도가 향상되고 압축항복강도가 증가하여, 강관의 붕괴성능이 향상되었다. 단, 강관의 직경/두께 비율에 따라 붕괴성능 향상에 미치는 Sizing 공정의 영향이 차이를 보였다. 탄성좌굴을 보이는 얇은 강관(즉, 직경/두께 비율이 큰 강관)에 대해서는 Sizing에 의한 붕괴성능 향상 효과가 미미하였다, 반면, 비탄성좌굴을 보이는 두꺼운 강관(즉, 직경/두께 비율이 작은 강관)의 경우에는 붕괴성능 향상에 미치는 Sizing의 효과가 지대하였다.

해석결과를 설계기준과 비교하여 붕괴성능에 미치는 Sizing 공정의 이점을 검토하였다. 강관의 붕괴성능에 대한 현재의 설계기준들은 Sizing 이 주는 이점을 고려하지 않고 있기 때문에, Sizing 공정의

이점이 큰 두꺼운 강관일수록 해석결과와 설계기준 사이의 차이가 점점 증가하였다.

본 연구 결과를 토대로 ERW 강관의 붕괴성능을 향상시키고 품질을 개선할 수 있는 ERW 강관 조관공정에 대한 유용한 데이터를 제공할 수 있을 것으로 기대된다.

주요어: ERW 강관, roll-forming 공정, sizing 공정, 유한요소해석, 진원도, 항복강도, 외압, 붕괴압력

학 번: 2015-30287